A TRIGGERED CLOUD CHAMBER INVESTIGATION OF HIGH ENERGY PHOTONUCLEAR REACTIONS.

by

BRANISLAV LALOVIC.

DEPARTMENT OF NATURAL PHILOSOPHY,
UNIVERSITY, GLASGOW.

Presented to the University of Glasgow, January, 1959
as a Thesis for the Degree of Doctor of Philosophy.

PREFACE.

This thesis is an account of the investigation performed at Glasgow University, between April, 1956 and July, 1958, under the supervision of Mr. J.R. Atkinson. The experiments which it describes were done by using, as a photon source, the bremsstrahlung spectrum of the 330 MeV. Glasgow University synchrotron. A triggered cloud chamber was developed and employed for the investigation of high-energy photonuclear reactions. The triggering pulses were provided by scintillation counter telescopes, which were set to detect high-energy protons produced by the X-ray beam in the cloud chamber gas.

In the introductory chapter, a survey of the work in the field of high-energy photonuclear reactions is given. Experimental and theoretical evidence, supporting the so-called quasi-deuteron model of photonuclear reactions, is presented. It is shown that the role of other possible mechanisms of γ-ray absorption at high energies has not been ascertained. Furthermore, in the case of the quasi-deuteron disintegration, the experiments performed so far have not provided data about the

angular distributions of protons and neutrons in the centre-of-mass of the quasi-deuteron. Data of this nature is needed to provide information about the nature of the short range pair correlations in complex nuclei. The triggered cloud chamber is shown to be able so supply some new information on these questions. The author's idea of using the recoil energy distribution for the measurement of internal momentum distribution is also explained.

In Chapter 3, the experimental apparatus is described. The cloud chamber used in this experiment was designed by Messrs. J.R. Atkinson and J.M. Reid. The author contributed to the development of some details such as the expansion system, spark valve, clearing field, illumination system, etc. The chamber was triggered by means of three scintillation counter telescopes using plastic scintillators. The author was responsible for the design and construction of the telescopes and accompanying electronics, and these are fully described. Various problems - the calibration of pulse height $\propto$ particle energy, non-linearity of the scintillator response, sources of background, method of analysis of photographs, etc., are discussed.

The experimental results are presented and

discussed in Chapter 3. The experiments were performed in collaboration with Mr. J.M. Reid. The analysis of all photographs was done entirely by the author. The interpretation and discussion of results are also the author's independent work. Some of the calculations of the particle kinematics were done by Mr. J.M. Reid, with whom many discussions relevant to the work were held.

The experiments were done with helium, nitrogen and neon, as irradiated gases. Reactions yielding from one up to six charged fragments were found to be associated with the high-energy proton emission. In most cases a high-energy neutron was also emitted, in agreement with the quasi-deuteron model. The proportion of events in which the residual nucleus is left intact is much smaller than expected for light nuclei. A small number of events in which only a single proton was ejected as well as a few other events not explainable on the basis of the quasi-deuteron model, were also found. Recoil energy distributions in the case of (γ,pn) events were obtained, but the statistics attained were not sufficient to derive accurate values of the average internal momenta of nucleons.

APPENDIX.

At the end of the thesis, an appendix is added, in which the author's work in the Institute of Nuclear Sciences in Belgrade, done between 1952 and 1956, prior to his coming to Glasgow, is described. This work concerned studies of the operation of the diffusion cloud chamber and its automation, and also some measurements of neutron spectra by means of the scintillation counter technique. These experiments were done in collaboration with Mr. A. Milojevic, Mr. M. Cerineo and Mr. F. Boreli and were reported in the Bulletin of the Institute, "B. Kidrich", and in "Nature".

ACKNOWLEDGMENTS.

This work was done while the author held a Fellowship of the European Organisation for Nuclear Research, (C.E.R.N.).

The author also wishes to thank: Professor P.I. Dee for extending to him the facilities of research at Glasgow University and for his interest in this work; Mr. J.R. Atkinson and Mr. J.R. Reid for their support and helpfull co-operation; Mr. R. Turnbull for assistance in the experimental work and in language difficulties in writing this thesis; Miss M. Hughes for typing the thesis; Dr. McFarlane and Mr. T. Elder who operated the synchrotron.

I would also like to express my gratitude to the whole family of Dr. K. Matthew whose warm hospitality and friendship much facilitated my stay in Scotland.

The author is further indebted to Professor P. Savich and Dr. A. Milojevich for their support and sustained interest in the author's studies from the beginning of his work in the Institute of Nuclear Sciences in Belgrade.

CONTENTS.

CHAPTER I.

REVIEW OF THE EXPERIMENTAL AND THEORETICAL WORK ON THE HIGH ENERGY PHOTONUCLEAR EFFECT.

Introduction.

Gamma rays were used to produce nuclear photo-disintegration for the first time in 1934, when Goldhaber and Chadwick (1) demonstrated the break-up of deuterons under irradiation by ThC" 2.62 Mev γ-rays. From this experiment they were able to derive important data on neutron mass and deuteron binding energy. Almost at the same time Szilard and Chalmers (2) showed that neutrons were also produced when beryllium was exposed to the same irradiation. In this way, a new field of investigation in nuclear physics, that of photonuclear reactions, was opened.

However, further progress was hindered by the low energies and intensities of the γ-rays of the natural radioactive elements, the only photon sources then available. An advance came when high tension accelerators were employed to produce nuclear reactions in which γ-rays of higher energies were emitted. Several such reactions were exploited, particularly the reaction $Li^7(p,\gamma)Be^8$, which provided γ-rays of

17.7 and 14.8 Mev. This reaction was used by Bothe and Gentner (3) to study the cross-sections of (γ,n) reactions in several elements, and also by Huber and al. (4) to demonstrate a (γ,p) reaction in a nucleus more complex than the deuteron. At the same time as this experimental work a basis for the theoretical investigation of the photonuclear effect was laid down by Bethe and Peierls (5,6).

Following this pioneering work an increase in the interest in photonuclear reactions came with the development, from 1941 onwards, of electron accelerators; betatrons, synchrotrons and the linear type. Those machines, capable of producing bremsstrahlung spectra of high intensities and variable peak energies, greatly enlarged the scope of the investigation in this field. Many different photonuclear reactions have been observed and studied in detail and important discoveries, such as the giant resonance in photon absorption, the photodisintegration of "quasi-deuterons" in complex nuclei, etc., were made. With energies above 140 Mev the photoproduction of mesons became possible, and hence a new field, of photomeson physics, was established. Electron acceler-

ators of energies up to 1 Bev have been built, and today the study of photonuclear processes constitutes an important part of nuclear research.

In the present work photonuclear reactions at photon energies above 100 Mev are investigated. In virtue of the complicated nature of these processes and the complex character of the bremsstrahlung spectrum, the experimental study of the high energy photonuclear effect presents a difficult problem, and the data accumulated so far is not very extensive. The present experiment is an attempt to apply the method of the triggered cloud chamber to this investigation in order to supplement the information obtained by other techniques.

In this chapter a detailed review of the present state of the experimental and theoretical work on the high energy photonuclear effect is presented. The work at low energies is referred to briefly only, merely for the purpose of presenting a more complete picture of the whole field of the photonuclear effect. The photomeson processes, although they occur at energies in which we are interested, lie beyond the scope of the present investigation and are omitted

from this discussion.

1. The low energy photonuclear effect.

For photon energies below about 30 Mev much experimental work has been done and comprehensive data has been accumulated. The energy dependence of cross-sections and the angular distributions of reaction products have been measured for many different photo-reactions throughout the periodic system. The most interesting feature in this energy region is the existence of the so-called giant resonance. Baldwin et al. (7) were the first to observe, in experiments using a 100 Mev betatron beam and the photonuclear plate detection technique, that the yield of (γ,n) reactions exhibited a broad peak at about 20 Mev. Subsequent measurements by many other workers have revealed the following basic facts about this resonance:

(a) All elements exhibit this resonant behaviour.

(b) It is present in all types of photonuclear reactions.

(c) The γ-ray energy at the peak of the resonance is about 22 Mev for lighter elements and falls off, as $A^{-0.2}$, (A = atomic number), to about 14 Mev for heavier elements. The width at half

of the peak amplitude is 6 - 8 Mev. The peak cross-section is of the order of 0.1 barn.

(d) The giant resonance absorption has almost entirely electric dipole character.

Above the giant resonance the cross-sections drop to much lower values.

Two basically different models, each having several variants, have been proposed to explain the giant resonance data. On one side it is supposed (8,9,10) that the nucleus as a whole interacts with photons (collective models). The giant resonance in these models is a result of the excitation by the γ-rays of the collective oscillation of protons against neutrons. In the opposite model, single nucleons are taken as responsible for photon absorption (single nucleon model) 11,12). In this case, it is shown by using the shell model data on nuclear levels, that the dipole transitions cluster around a certain mean γ-ray energy, giving rise to a resonance in the yield curve. It will only be mentioned that both models give predictions which are more-or-less in general agreement with the experimental data, each having some advantages on certain points.

One can also draw some general conclusions about the interaction of electromagnetic radiations with nuclei without relying on any specific model. On the basis of general quantum-mechanical results the following expression is obtained for the integrated cross-section for electric dipole absorption of photons by a nucleus containing N neutrons and Z protons (13):-

$$\int \sigma_\tau \, dW = \frac{2\pi^2 \hbar e^2}{M c} \frac{N Z}{A} (1 + 0.8x) \text{ Mev-barn} \quad \ldots\ldots(1)$$

where σ_τ is the total cross-section for the absorption of photons of energy W, and M is the nucleon mass. Factor x represents the relative contribution of the exchange of mesons to the nuclear force.

The above result is derived by using the sum rule for the electric dipole transition matrix elements. This rule, originally derived for the case of electrons in an atom, states that the sum of the squares of matrix elements for the transition between ground state 0 and all other states n is proportional to the number of electrons Z. When applied to the nucleus the sum equals $Z \frac{N}{A}$, the remaining part of the transition $(1 - \frac{N}{A})$ being connected with the centre-of-mass motion of the nuclear recoil.

Equation (1) implies the integration over all photon energies. It should then be possible to estimate

the contribution of higher energies to the dipole sum. A calculation on the basis of known cross-sections for various reactions at low energies shows (13,14) that the giant resonance almost "exhausts" the dipole sum, thus indicating very small cross-sections at high energies.

However, it should be borne in mind that the dipole sum includes only the conventional electromagnetic interaction, i.e., it ignores dipole transitions connected with the creation of mesons. The photon absorption above 100 Mev, however, is found to be mainly a meson connected process,including reactions in which mesons are not emitted. Therefore, the dipole sum is not of much concern to higher energies, even though the γ-ray absorption there is also predominantly of the electric dipole type.

2. The photonuclear effect at high energies.

At γ-ray energies above the giant resonance the energy available in the reaction is sufficient for the emission of several particles, and hence the nucleus can be split in many different ways. The experiments have confirmed, indeed, that the creation of "stars" is the most common type of event resulting from the absorption of high energy photons. However, early experiments at higher energies also showed an appreciable emission of high-energy nucleons. Thus Walker (15) found,using the nuc-

lear emulsion technique for proton detection, that protons of energies up to 124 Mev were emitted from carbon irradiated by a 195 Mev bramsstrahlung spectrum. The proton spectrum was found to be of the form $N=NE^{-n}$, where $n = 4$, with an even stronger falling off above 100 Mev, i.e.,at half the maximum γ-ray energy. The proton angular distribution showed a strong forward peak. Walker came to the conclusion that these features could not be explained on the basis of a compound nucleus picture or direct photonucleon emission and that they were in accordance with an assumption that γ-rays were absorbed by pairs of nucleons. Levinthal and Silverman (16) also measured the energy and angular distribution of protons ejected by high energy γ-rays.They used a bremsstrahlung of 320 Mev peak energy and proportional counters as proton detectors, and also found a forward assymetry in the angular distribution and a falling proton spectrum. The results were compared with a calculation of direct photonuclear effect, and an agreement was found in the cross-section for a proton energy of 40 Mev. However,protons were supposed to have high components of initial momenta in the nucleus, not appropriate to a Fermi gas of nuclear density. Nucleons would have such high momenta only if there existed short range nucleon correlations. On the basis of these experimental results,

Levinger (17) proposed that high energy γ-rays interact with proton-neutron pairs, called quasi-deuterons, when the two nucleons are found at close mutual proximity inside nuclei. Hence in such a process protons and neutrons should be emitted in coincidence, and their kinematics should resemble that of the photodisintegration of free deuterons. This prediction was immdeiately confirmed by experiments. Barton and Smith (18) at Illinois and, at the same time, Wattenberg et al. at Massachussetts, observed n-p coincidences from several light elements, using bremsstrahlung spectra of 265 and 325 Mev, respectively, and scintillation counters for detection of protons and neutrons. Barton and Smith estimated that about 53 percent of all high energy protons from lithium had a correlated neutron, and when the interaction of neutrons in the nucleus, subsequent to the absorption of the γ -ray, was taken into account, the possibility remained that all high energy protons were produced in a two-body photodisintegration. Similar conclusions were also reached by the Massachussetts group (19).

Later, a more extensive investigation of the

coincident emission of protons and neutrons was performed by both these groups. Wattenberg et al. (20) measured n-p coincidences from Li, C, O, Al, etc., using bremsstrahlung of 325 Mev. In these experiments a proton telescope was placed at a fixed angle of 70° with respect to the γ-ray beam, while the angle of a neutron counter was varied. The proton energy was also held fixed at 120 Mev, and the neutron energy was only known to be higher than 15 Mev. Curves of the n-p angular correlation were obtained, and a direct comparison with similar curves for deuterium was made. Neutrons were found to have an angular spread around that mean angle in which they would have travelled had they been emitted in the photodisintegration of free deuterons. This spread was attributed to the influence of the nucleon internal momentum, i.e. to the fact that p-n pairs are not stationary in the instant of their interaction with γ-rays. Consequently these data were used to calculate the average internal momenta of nucleons in nuclei. The experimental results were found to fit a three dimensional Gaussian distribution with 1/e values of 9, 19, and 19 Mev. for

Li, C, and O, respectively.

The measured values of the cross-sections for the observation of n-p coincidences for elements from Li to Pb were found to agree with a formula of the type which Levinger had derived:

$$\sigma(Z^A) = C\ NZ/A\ \sigma_d\ f(2R/\Lambda) \qquad (2)$$

where C is a constant with a value of 4 ± 1, N and Z are the numbers of protons and neutrons, respectively, and σ_d is the observed cross-section for the photo-disintegration of deuterium; $f(2R/\Lambda)$ is a calculated attenuation factor which gives the probability of escape of neutrons and protons as a function of the nuclear radius R and mean free path Λ of nucleons in nuclear matter. $f(2R/\Lambda)$ was estimated to be about 40 percent for C and 7 percent for Pb.

Barton and Smith (21) measured correlated n-p pairs from Li and He, and found that simple Levinger theory can be used to explain the basic features of this process. They also convinced themselves that "almost all" high energy protons were ejected in two-nucleon disintegration. However, they derived a value for the internal momentum in lithium (1/e value = 5 ± 1 Mev) which differed appreciably from the value

found by Wattenberg et al.

Several other experiments have also produced evidence that the absorption by two nucleons represents the main process of photon absorption in complex nuclei. Gorbunov and Scherbakov (22) performed an experiment on the photodisintegration of helium, by using a cloud chamber with a magnetic field and 240 Mev bramsstrahlung. They found that at photon energies up to 150 Mev the angular distribution and proton-neutron correlation in the reaction $He^4(\gamma,pn)H^2$ showed characteristic features of the two-nucleon disintegration. Photoneutrons emitted from deuterium and carbon were investigated by Baranov et al. (23), and the ratio of the cross-sections for these two elements was found to be in agreement with the Levinger quasi-deuteron model. It is interesting that the same ratio was found for maximum photon energies of 170 and 255 Mev, but only in the second case were the neutrons accompanying the photomeson production, detected.

It is of interest to know the lower limit of γ-ray energy at which the two-nucleon model is still valid. The measurements of photoproton emission below 100 Mev

were done by Chuvillo and Schevchenko (24, 25), (nuclear emulsion technique), Whitehead et al., (26), Johansson (27) and Bazdanov et al. (28), (scintillation counter technique). Chuvillo and Schevchenko's results showed that the emission of fast protons from beryllium at $E_{\gamma\,max.} = 84$ Mev and $E_{\gamma\,max.} = 65$ Mev was in accordance with the quasi-deuteron model, but in the case of carbon at $E_{\gamma\,max.} = 65$ Mev an absorption into α-particle subunits seemed more probable. Johansson concluded from his experiment, that the emission of protons and neutrons from carbon at this energy could be explained on the basis of the independent particle model. Whitehead et al., found that the principal contribution to the cross-section for proton emission from carbon, beryllium and lithium came from quasi-deuteron interactions. The measurement of protons from Al and Ni for $E_{\gamma max} = 100$ Mev, of Bazdanov et al., indicated a discrepancy with the two-nucleon model only for big angles of proton emission. Thus, it seems that even at intermediate energies the quasi-deuteron interaction might be of importance, but its relative role seems to depend on the individual characteristics

of the element studied and the isotopic selection rule may have an important influence. However, more experimental data is needed before definite conclusions can be drawn about the mechanisms of the photonuclear interaction in this transitory region.

Although multiple particle emission is typical for high energy photodisintegration, this type of event has been least investigated and the mechanism of star production is not known for certain yet. Stars can be the result of compound nucleus formation, but the cross-section for this process is considered negligible at higher energies. The production of mesons and their re-absorption in the same nucleus can be responsible for the creation of stars. Such a process will leave the nucleus with an excitation energy above 150 Mev and hence an emission of several particles is made possible. The absorption of γ-rays by quasi-deuterons can also lead to the creation of stars. This will happen if the nucleons are scattered or absorbed on their way out of the nucleus. In addition, the residual nucleus can be left with a high excitation energy purely as a consequence of the removal

of two nucleons from the original structure.

Kikuchi (29) investigated stars created in nuclear plates by a 300 Mev bremsstrahlung beam and found the total cross-section for all stars to be of the same order of magnitude as for photomeson production. Miller (30) similarly studied multiprong events by using bremsstrahlung spectra of 161, 242 and 322 Mev. He found an increase in the cross-section above the meson threshold and reported a value of $8.10^{-27} cm^2$ for the average cross-section for the production of more-than-three-prong stars at photon energies betweeen 242 and 322 Mev. This is a value several times greater than the photomeson production cross-section, and Miller suggested that it could be a result of strong reabsorption of mesons. This conclusion is supported by the fact that the meson yield per nucleon is found to be proportional to $A^{-1/3}$, which indicates that only surface nucleons are effective in producing mesons, whilst mesons produced in the interior are mostly reabsorbed. Peterson and Roos (31) derived a similar conclusion from their experiment measuring the energy dependence of the star production for photon energies from 250 up to 500 Mev. The cross-section found for silver was about 100 times higher than the free nucleon

photomeson cross-section. From this result they derived a value of 1.10^{-13} cm. for the mean free path of pions in nuclear matter. However, since this is shorter than the average inter-nucleon separation, it might be considered that the meson is re-absorbed mostly within the volume of the pair of nucleons in which it is created. Thus one essentially arrives at the quasi-deuteron model of γ-ray absorption. However, further more accurate and extensive measurements are required to clarify this question.

Although there is convincing evidence that high energy γ-rays are predominantly absorbed by p-n pairs in complex nuclei, the experimental results are still uncertain by a large factor. The measurements of the n-p coincidences had to be corrected for the internal scattering of nucleons, and this could only be estimated with an uncertainty of about $\pm$ 25 percent. In addition, an accurate knowledge of the efficiency of the neutron counter was required, but this could not be precisely determined for an unknown complex neutron spectrum. Hence the exact role of other possible mechanisms of γ-ray absorption, such as the direct nucleon ejection, compound nucleus formation and meson

re-absorption, is still to be determined. The problem of the origin of "stars" also has to be ascertained. In addition to these questions it should be mentioned that very little is known about the excitation of the residual nucleus in high energy nuclear interactions which have localized character. One should expect the residual nucleus to be often left in a state rather different than its ground state and with a considerable excitation energy, but, for the sake of simplicity, this is usually neglected in theories and in the interpretation of experimental results. The present work in which a triggered cloud chamber is employed is aimed at supplying certain information about some of these problems as will be described in Section 3 of this chapter.

While the kinematics of the disintegration of p-n pairs in complex nuclei has been studied, the deeper, dynamical aspect is yet to be investigated. It would be of great interest to acquire some information about the short range proton-neutron correlation function in complex nuclei, and to compare it with the free deuteron state. To obtain this important data a knowledge of the angular distributions of nucleons in the centre-of-

mass of the quasi-deuteron is required. In counter experiments this is difficult to achieve because of the lack of information about the quasi-deuteron internal momentum in the case of any particular event, and also because of the uncertainty brought about by the internal scattering of nucleons. In order to overcome this difficulty one has to measure both proton and neutron energies and directions of emission, and also to separate these two effects. However, the measurement of neutron energy with a reasonable efficiency in this energy region has not yet been achieved, and hence the development of other techniques which may be useful in this respect is demanded. In the next section it will be shown how the method to be described here, can contribute to the solution of this problem.

3. Experimental techniques in the investigation of high energy photonuclear reactions.

(a) Scintillation and proportional counters.

Scintillation counters have been extensively used for the detection of high energy particles, e.g. protons, neutrons, mesons, etc. In the case of protons and mesons, scintillation counter telescopes, consisting of two or more counters set in coincidence, can be used to

determine, with good precision and a hundred percent efficiency, the particle nature and energy. In these telescopes one counter is usually used to measure the energy loss per unit length, dE/dx, and this provides information about the nature of the particle. The particle energy is defined by its range, which is known from the pulse height in the last counter. In the case of simple processes, such as the photomeson production in hydrogen, the photodisintegration of deuterium, etc., a telescope of this kind provides all the necessary information about the reaction. However, when one deals with photonuclear reactions produced by a bremsstrahlung beam in complex nuclei, where events are more complicated, the detection of only one particle appears to be insufficient. Even in the relatively simple case of the quasi-deuteron photodisintegration, one has, as it was mentioned in the previous section, to detect both proton and neutron and to measure their directions and energies, in order to obtain all the required data.

High energy neutrons can be detected with an efficiency up to 10 percent by using a large volume of

a suitable scintillator. The measurement of neutron energy, however, is a more difficult problem. A promising technique in this respect is the time-of-flight method, the application of which to high energies has recently been made possible by the development of electronic circuits with resolving times better than 10^{-9} sec.

Proportional counters are also used for the detection of protons and other heavier particles. They are more suitable at lower energies and are particularly useful when one has to distinguish among deuterons, tritons, α-particles etc. They can also be used in combination with scintillation counters. In comparison with the latter, proportional counters are at a disadvantage with respect to the resolving time; this is of the order of a microsecond in proportional counters as compared to a millimicrosecond in scintillation counters. It may be added that the counter technique is not suitable for the study of multiple particle emission.

(b) Photonuclear plates.

In photonuclear experiments the photonuclear plates can either be directly irradiated or exposed to

fast particles originating in an external target. In the former case all charged particles except the low energy ones and heavy recoils are detected. The type of particle can often be recognised, but the accuracy of the energy measurement is not good at higher energies. The presence of several elements in the emulsion introduces some uncertainty in the interpretation of events and a further disadvantage is the strong ionization of the γ-ray beam, which limits the time of the irradiation. Direct irradiation has been shown to be very useful in the study of stars. The detection in plates of high energy particles from an external target is justified when very low yields are encountered but the technique of plate scanning is slow and tedious in comparison with counter detection.

An important disadvantage of plates is that they neither record neutral particles nor heavy recoils.

(c) Induced radioactivity.

This method has very limited applicability at higher energies since only a very small proportion of reactions leads to suitable radioactive products. In addition, in virtue of the low cross-sections at higher

energies, the yields are usually very small.

(d) Bubble chambers.

This new experimental technique, which has found a wide application in high energy physics, has not been much used in the study of photonuclear reactions. In principle, a bubble chamber could be very useful as a liquid target with a relatively high stopping power for particles emitted from a reaction. It offers a possibility of recognizing the nature of the particles and of measuring their energies from the bubble densities. However, only very low beam intensities can be put through the chamber liquid if excessive ionization is to be avoided. This reduces the number of high energy events obtained per beam pulse.

(e) Cloud chamber.

The cloud chamber has been very useful in photonuclear investigations, especially at low photon energies. The low stopping power of the chamber gas makes possible the detection of low energy particles and even heavy nuclear fragments. At low energies, the ranges and hence the energies of particles as well as their directions can be measured. At higher energies a

magnetic field must be employed to measure the energies of particles not stopping in the chamber gas. In this way the use of the cloud chamber can be extended to a photon energy of about 100 Mev. However, for photon energy above 50 Mev the photodisintegration cross-section drops to about 0.1 millibarn, and the number of events produced in the gas becomes extremely small. Therefore the use of cloud chamber with a magnetic field is restricted to the intermediate energy region.

For high photon energies a triggered cloud chamber can be used in conjunction with scintillation counters. These can be employed to detect high energy particles originating in the chamber gas, and the pulses so obtained used for the triggering of the chamber. The cloud chamber photograph would then show the type of event leading to the emission of the triggering particle, the number of other charged particles emitted, their directions, ranges of those which stop in the gas, momentum "unbalance", etc. Hence by this technique information not obtainable from counter experiments can be obtained.

For example, if the counters are set to detect high energy protons, the following data can be obtained

from the photographs. In the first place, the triggering proton can readily be shown to be directly and solely ejected or to be accompanied by a neutron, depending on whether the recoil is or is not coplanar with the proton and γ -ray. The range of the recoil is a confirming factor in the case of coplanar events that direct ejection in a (γ,p) reaction is the correct interpretation. Secondly, in the case of (γ,pn) events, it supplies information about the neutron energy as well as its direction. This, with the knowledge from the counters of proton energy and with the proton angle as measured in the chamber, specifies the event completely, and in particular enables the γ -ray energy to be evaluated. Furthermore, if the quasi-deuteron model is valid for these ((γ,pn) type) events, the observed residual nucleus must be recoiling with exactly the opposite momentum to the quasi-deuteron which has been photodisintegrated. Hence the range distribution of the recoils represents directly, with very little correction, the internal momentum distribution of deuterons. It should be further noted that the deuteron internal momentum is known for each particular

event and consequently there exists the possibility of deriving the angular distribution corrected for deuteron internal momentum and with the certainty that only those events are being included in which proton and neutron escape from the nucleus without an intensive interaction with other nucleons.

The recoil energies of light elements can be estimated from the cloud chamber photographs down to an energy of 1 Mev, with an error not exceeding $\pm$ 10 percent. Hence, the accuracy of this method of measurement of the internal momentum distribution can be comparable to the counter method.

The main difficulties of the triggered cloud chamber method are: (a) the fast triggering particle must be photographed in the presence of an intense ionization accompanying the passage of the γ -ray beam, (b) the method is restricted to gas targets and therefore good statistics require a lengthy experiment; and (c) the geometry of the experiment is very involved, thus making difficult an accurate measurement of the cross-sections and angular distributions.

4. Theories of the high energy photonuclear effect.

(a) The photodisintegration of deuteron.

Since the photodisintegration of p-n pairs in complex nuclei is closely related to the photodisintegration of the deuteron, it is of interest to review first the present knowledge of this latter process.

The photodisintegration of deuterium has been extensively studied for photon energies from the threshold up to several hundred Mev, and the cross-sections as well as the angular distributions are known over this whole energy region. This data shows four distinctive regions:

(1) Just above threshold the absorption is found to be predominantly of magnetic dipole type. The cross-section for this absorption reaches amximum at about 65 Kev above the threshold and then falls off rapidly, becoming negligible for $E_\gamma > 3$ Mev.

(2) For $3 < E < 10$ Mev the electric dipole becomes the most important transition. The cross-section rises to maximum at $E_\gamma = 4.5$ Mev, when it has a value of 25.10^{-28} cm.^{2}, and at higher energies falls off as $E^{-3/2}$. The angular distribution is of $\sin^2\theta$ type

(in the centre-of-mass system).

(3) For $10 < E < 100$ Mev the total cross-section declines steadily, reaching a value of 70 microbarns at $E_\gamma = 100$ Mev. The angular distribution becomes assymetric around 90° and, in addition, a strong isotropic term appears. Electric quadrupole also becomes of importance, and it is an interference between electric dipole and electric quadrupole transitions which causes the assymetry in the angular distribution.

(4) For photon energies above 100 Mev there is little change in the cross-section until meson threshold is reached. Then the cross-section starts to rise until a maximum at about 250 Mev is attained. At this energy $\sigma_t = 60.10^{-30} \text{cm.}^2$, i.e., it is of the same order of magnitude as the photomeson production cross-section. The assymetry as well as the isotropic term become remarkable, and $\sin^2\theta$ term is decreased.

Although the deuteron is the simplest nuclear system, the theoretical treatment of the deuteron photodisintegration presents a difficult problem, which has been satisfactorily solved only for low photon energies. The main reason for this lies in the fact that the nuclear forces are partly due to the exchange of mesons,

and the exact nature of this is not adequately understood. Hence no complete treatment of the interaction of electromagnetic radiation with nuclei, which includes the meson exchange current, has been developed. However, it has been shown that for photon energies below 50 Mev one can ignore the meson connected effect in electric dipole transitions, and use the conventional theory of nuclear forces (Siegert theorem).

For photon energy up to 10 Mev the effective range theory of nuclear forces is applied. The ground state of deuteron is known to be a ^3S state with 5 percent admixture of ^3D state, and the ground state wave function can be set up. The dipole transitions proceed mainly via $^3S \longrightarrow {}^3P$ transitions and in the effective range approximation the interaction of p-n system in the final ^3P state is considered negligible. The theoretical results are in satisfactory agreement with the experimental facts.

Schiff, Marshal and Guth (32) have extended this theory to a photon energy up to 150 Mev, but their results for the cross-section above 50 Mev are much smaller than the experimental values. There is also a

discrepancy between the angular distributions predicted by this theory and the observed distributions; the theory does not predict an isotropic term.

A theory which achieves a reasonable agreement with the experimental data up to photon energy of 150 Mev has recently been developed by de Swart and Marshak (33). This theory also relies on the Siegert theorem, but it uses a different wave function for the deuteron ground state, which has a 7 percent admixture of D state. An appreciable isotropy in the angular distribution is obtained as a result of an interference of $^3F_2$ with ^3P final states.

At photon energies above meson threshold the mesonic effects play an important role and Siegert theorem is no longer valid. It was first proposed by Wilson (34) that meson production and reabsorption is responsible for the relatively high value of the deuteron photodisintegration cross-section at high energies. According to Wilson's idea, when a meson is created in a deuteron it has a chance either to escape from the deuteron or to be reabsorbed within it. This latter has a high probability if the neutron and proton

happen to be within the range of the nuclear force $h/\mu c$ ($\approx 10^{-13}$cm.). In this case, the meson total energy goes over to the kinetic energy of the two nucleons.

Wilson's theory was further elaborated by Feld (35) and, independently, by Austern (36). They applied the isobaric model of nucleon to calculate the above effect. According to this model a nucleon which absorbes a photon is lifted into a quasistable isobaric state, characterized by total spin J = 3/2 and isotpic spin T = 3/2. This state can decay in one of the following ways:-

$$\gamma + D \rightarrow N + N^{*} \rightarrow N + N$$
$$\rightarrow N + N + \pi^{o}$$
$$\rightarrow N + N + \pi^{+,-}$$
$$\rightarrow D + \gamma$$

Reciprocating, the same intermediate state is involved in the (π^{+},p) scattering (cross-section σ_2), in (γ,π^{o}) photoproduction in hydrogen, (cross-section σ_3) and in π^{+} disintegration of deuterium (cross-section σ_4). Then it can be shown that the cross-section (σ_α) for the photodisintegration of deuterium is related to these processes in the following way:-

$$\sigma_d = (9/4)\ \sigma_3\ \sigma_4 / \sigma_2$$

Cross-sections σ_2, σ_3 and σ_4 are known from separate experiments, so that σ_d can be calculated from the above formula. Such calculation gives a broad resonance above meson threshold, in qualitative agreement with the observed trend in the cross-section. But in absolute values the cross-section is only about half that found experimentally. The expected angular distribution is of the form $(1 + 3/2\sin^2\theta)$, which, again, only qualitatively approaches the experimental data.

It should be noted that meson production and reabsorption can play a certain role even below meson threshold. In this case, of course, only virtual mesons come into consideration. Wilson (37) has shown that virtual mesons produced in S state contribute considerably to the deuterium photodisintegration cross-section.

(b) Photodisintegration of complex nuclei.

The experimentally observed fact that high energy γ-rays are predominantly absorbed by p-n pairs can be easily understood in a qualitative way. At high energies two basic features of γ-rays play a

decisive role in the photonuclear interaction. Firstly, the wave length of high energy photons is smaller than nuclear diameters. For example, the wave length of a 300 Mev photon is equal to one ninth of the diameter of nitrogen. Therefore, one can generally expect that the photonuclear interaction will affect only a small part of the nucleus. In fact, one can say that a high energy photon sees nucleons in a nucleus as independent units.

On the other side, photons, by their nature, carry high energy with little momentum. For instance, a 300 Mev photon has the same momentum as 50 Mev nucleon. Because of such combination of the momentum and energy, the possibility of transfer of photon energy to individual nucleons is restricted. Such a transfer can proceed via Compton scattering on nucleons, but the cross-section for this process (10^{-31} cm^2 at 100Mev) is by a factor of 10^3 smaller than the cross-section for the photoproduction of high energy nucleons. In addition, Compton scattering cannot produce nucleons at backward angles.

Direct ejection of single nucleons from nuclei is possible only if nucleons have high momenta in their initial states. For, only high momentum

components in the wave function of the initial state appreciably contribute to the transition matrix elements, the square of which is proportional to the cross-section. However, the probability of having high momenta in a Fermi gas of nuclear density is very small. Only when nucleons happen to be at mutual distances much smaller than the average internucleon separation they will have high momenta. If the probability of finding more than two nucleons at such short separation is considered negligible, a conclusion can be derived that high energy γ-rays will be predominantly absorbed by two nucleons which are found at close proximity inside a complex nucleus. Since, furthermore, the photonuclear interaction at the energies considered is believed to be predominantly of the electric dipole type, and neither two protons nor two neutrons have an electric dipole moment , only proton-neutron pairs can appreciably contribute to the γ-ray absorption.

This conclusion is also valid if meson production and reabsorption within p-n pairs is assumed to be the main mechanism of the γ-ray absorption. In this case

also, as it was noted in the previous paragraph, the meson will be reabsorbed only if the two nucleons are within a distance shorter than the range of nuclear forces, which is smaller than the average separation of nucleons.

Levinger (17) was first to derive an expression for the cross-section for the quasi-deuteron photodisintegration. He assumes that the ground state wave function of a nucleus can be written as a product of function $\psi_k(r)$ describing the p-n pair and a function $\varphi(3...A)$ for the remaining A-2 nucleons:

$$\psi(1, 2, 3...A) = \exp(i\underline{k}'\underline{r}')\,\psi_{k'}(\underline{r})\,\varphi(3...A)$$

where the term exp(ik'r) describes the motion of the centre-of-mass of the quasi-deuteron. Assuming further that the initial and final states of A-2 nucleons are same and using the effective range theory of nuclear forces, Levinger was able to show that the wave function $\psi_k(r)$ of the quasi-deuteron is a multiple of the free deuteron wave function. Then the following ratio of the cross-sections for the photodisintegration of quasi-deuterons and deuterons, respectively, is

derived:-

$$\frac{\sigma_{2d}}{\sigma_d} = \left(\frac{\psi_k}{\psi_d}\right)^2 = 2\pi(1-\alpha r_0)/\alpha(\alpha^2+K^2)V$$

Here:- $\alpha = k \cot\delta$ = scattering length, where δ is the phase shift and $k = \frac{1}{2}|\underline{k}_1 - \underline{k}_2|$ is the momentum or relative motion of p-n pair; r_o is the effective range of nuclear forces; V is the volume of the nucleus.

The ratio given by equation (3) was calculated by assuming Fermi distribution for the nucleon internal momentum and takin average of $(a^2 + k^2)^{-1}$ over all possible values of k. As a result a simple formula was obtained:

$$\sigma = 6.4\left(\frac{NZ}{A}\right)\sigma_{dth} \qquad (4)$$

where σ_{dth} is the theoretical value of the deuteron photodisintegration cross-section, calculated on the basis of conventional theory of nuclear forces. The proportionality factor C = 6.4 represents the probability, relative to deuteron, of having high initial momenta of nucleons in the quasi-deuteron.

The prediction of NZ/A dependence in the above

formula (NZ = number of p-n pairs, A~ volume of the nucleus) is confirmed experimentally. The absolute values of the cross-section, however, are much smaller than the experimental values, mainly because $\sigma_{d\,th}$, as used above, is smaller than the experimental values, of $\sigma_{d\,exp}$. By using this latter, a better agreement with the experimental results could be achieved. However the photodisintegration of deuterium at higher energies is found to be a meson connected process and such a use (of $\sigma_{d\ exp.}$ in Eqn. (4)) is not justified since Levinger treatment includes no reference to mesons.

The interaction of proton and neutron with the residual nucleons after the absorption of γ-ray is ignored in Levinger's derivation. This, however, is very serious even in the lightest nuclei, and has to be taken into account. For example, in the case of oxygen the chance that both particles escape without interaction is only 30 percent.

A more elaborate and comprehensive theory of the quasi-deuteron photodisintegration was given by Gottfried (38). In this theory the wave function for a pair of nucleons in a complex nucleus is written as:-

$$\rho(\underline{r}_1, \underline{r}_2) = \rho_s(r_1, r_2) / g(|\underline{r}_1 - \underline{r}_2|)^2 \qquad (5)$$

Here ρ_s is the correlation function resulting from the correlations due to Pauli principle and to the finite size of the nucleus; the correlation due to the short range nuclear force is represented by g. Further assumptions of this theory are: (a) the photonuclear interaction is taken to be a meson connected process and three nucleon effects are considered negligible; (b) the influence of the remaining A-2 nucleons during the absorption act is neglected (impulse approximation); (c) the excitation energy of the residual nucleus is supposed to be small compared with photon energy, and (d) transitions from initial S-singlet state are neglected.

Under these assumptions the following formula is derived for the cross-section:

$$d\sigma = (2\pi)^{-4} F(P)\, S_{fi} \cdot \delta(E_f - E_i)\, d^3k_1 d^3k_2 \qquad (6)$$

where: F(P) - the probability of finding two particles (in the Slater determinant of the shell model) of zero separation and total momentum P;

S_{fi} - the sum of squares of transition matrix elements, for transitions from initial state defined by

function (5) to final two body scattering state;

k_1 and k_2 - momenta of the ejected nucleons.

Since the pair correlation function is not known, matrix elements S_{fi} cannot be directly calculated. This is overcome by supposing that for distances $r \leq 10^{-13}$ cm. the pair correlation function is proportional to the deuterium ground state wave function.

$$|g(x)|^2 = \gamma^3 |\phi_0(x)|^2 \qquad (7)$$

where γ is a constant. Then the following ratio between the photoeffects in complex nuclei and deuteron results:

$$\frac{d\sigma/d\Omega_p}{[d\sigma_D/d\Omega_p]_0} = \frac{3\gamma^3}{4\pi^3} F(P) \frac{K_p E_p}{[K_p E_p]_0} \delta(\varepsilon - \bar{\varepsilon})\, d\varepsilon_p\, d^3K_N \qquad (8)$$

where the deuterium cross-section is to be evaluated in the centre-of-mass frame defined by $(\underline{k}_p + \underline{k}_n) = 0$. It should be noted that this formula is valid only for nuclei having completely closed shells (e.g. O^{16}, Ca^{40}).

For practical purposes, where one deals with a bremsstrahlung spectrum, Gottfried calculates the ratio dR defined as:

$$dR = \frac{[\text{Coincidences/sec. between } (K_p K_N) \text{ and } (K_p + dK_p, K_N + dK_N)]_{\text{Nucleus}}}{\text{Coincidences/sec. between } K_p \text{ and } K_p + dK_p)_{\text{deuterium}}}$$

$$= \gamma^3/2\pi\, W(\underline{K}_p, \underline{K}_N)(\partial\omega_D/\partial\varepsilon_p)^{-1} I(\bar{\omega})/I(\omega_D)\, d^3K_N$$

where $I(\omega)d\omega$ is the number of photons incident per sec. per cm.^{2} in the interval $(\omega, \omega + d\omega)$, $\bar{\omega} = \varepsilon_N + \varepsilon_p + \bar{\varepsilon}$ with $\bar{\varepsilon}$ = binding energy plus an average of excitation

and recoil energy, and ω_D is the photon energy corresponding to k_p in the deuteron reaction, $W(\underline{k}_p , \underline{k}_n)$ represents proton-neutron angular correlation function, defined as:

$$W(\underline{K}_P, \underline{K}_N) = \tfrac{3}{2}\pi^2 F(P) \frac{K_P E_P}{[K_P E_P]_0} \frac{[d\sigma_P/d\Omega_P]_0}{d\sigma_D(K_P)/d\Omega_P} \qquad (10)$$

Gottfried has calculated the function $W(k_p, k_n)$ as well as the ratio (dR) for O^{16}, but they could not be compared with experimental data, since no measurements in which both proton and neutron momenta are defined had been performed. Such a comparison would particularly be important as a check of the validity of the assumption about the pair correlation function, contained in the ratio given by Eqn. (7). However, a certain comparison with experiments is possible if an integration over neutron energies of the ratio dR is carried out. Such a calculation, compared with experimental results for O obtained by the MIT group, (20) gave for the constant γ a value of approximately $5.1\ 10^{-13}$cm. The curve of proton-neutron angular correlation obtained after the integration over neutron energies agrees with the curve experimentally found.

The interaction of p-n pair with other nucleons

after the absorption of γ-ray is treated in Gottfried's theory by using the optical model of the nucleus. The interaction is considered to consist of two distinct processes: (1) absorption of the outgoing nucleons inside the nucleus, and (2) refraction of the outgoing wave by the imaginary part of the nuclear potential. The process (1) is calculated on the basis of mean free path of nucleons in nuclear matter, and (2) by using Born approximation. In this way two factors are obtained, by which the cross-section has to be multiplied.

It should be noted that both Levinger and Gottfried theories ignore the transitions from S-singlet state of the quasi-deuteron. This is justified by the fact that the photon absorption by free deuterons proceeds mainly (about 80 percent) via electric dipole absorption, whereas the transitions from the singlet state require an electric quadrupole absorption. In addition, the probabilities of singlet and triplet states are in ratio 1:3. However, the exact nature of γ-ray absorption by quasi-deuterons is not known since no data on the angular distribution of nucleons

in the quasi-deuteron centre-of-mass system are available. Therefore, the validity of this approximation can not be accurately judged.

Both theories also ignore the possibility that the residual nucleus can be left in a state different than its ground state and with a high excitation energy. There are no experimental data relevant to this question.

CHAPTER II.

EXPERIMENTAL TECHNIQUE.

1. The cloud chamber.

The cloud chamber used for these experiments was designed by Mr. J.R. Atkinson and Mr. J.M. Reid. The author contributed to the development of some details, such as the clearing field, illumination, spark valve, etc., and was responsible for the chamber operation in the course of the experiments.

The chamber is shown diagrammatically in Figure 1. It was a conventional square expansion cloud chamber of rubber diaphragm type, volume defined, with a sensitive volume of 30cm. x 30cm. x 15cm. On two opposite walls there were 8cm. diameter mylar windows of .001" thickness, for the passage of the γ-ray beam. Perspex windows for the illumination were made on the other pair of walls. The top of the chamber was covered with 2.5cm. thick armoured glass plate. The chamber was designed for operation with a compressed pressure of approximately 1.5atm

A clearing field was applied between two wire grids 10cm. apart, one grid being connected to +400V., the

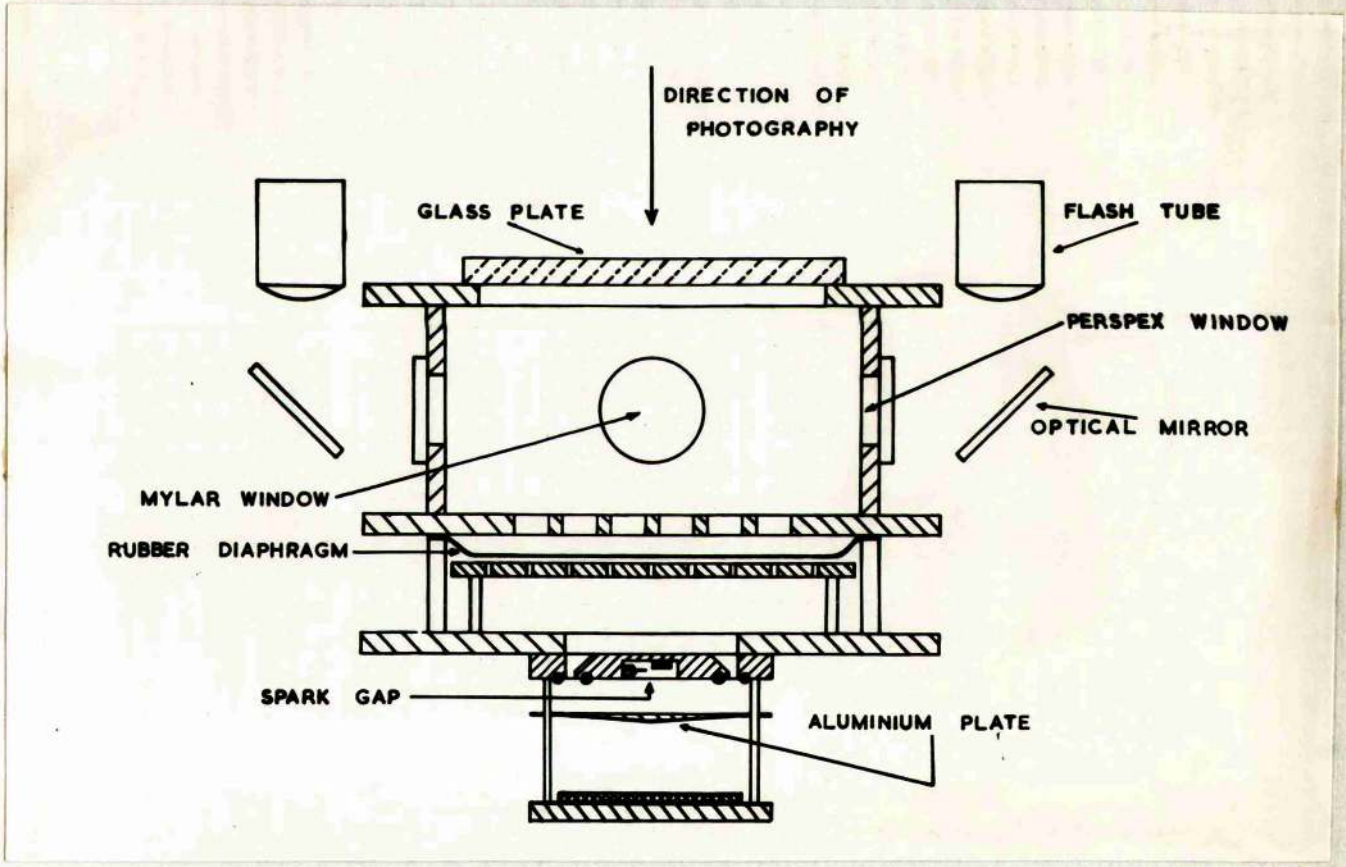

Figure 1.

Schematic diagram of the expansion cloud chamber

other to - 400 V. This high value of the clearing field was found necessary to sweep away the ions from one burst of quanta before the arrival of the next burst 1/5th sec. later. It was thus found possible to allow the machine to pulse regularly at a recurrence of 5/sec. until such time as a proton was emitted. To prevent the drawing of the tracks, should an expansion occur, an electronic switch was designed to earth both grids 5 m. sec. before each beam pulse and to restore the voltage 20 m.sec. after the pulse.

The circuit diagram of this switch is shown in Figure 2. A multivibrator, consisting of valves V_1 and V_2, produced a positive and negative pulse after being triggered by the pulse from the counters or from the synchrotron. The length of these pulses could be varied from 10 to 50 m.sec. The positive pulse was led to the valve V_3 and the negative one to the valve V_4. The clearing voltages +400 and -400V. were at the same time the operating voltages of these valves. The negative pulse from the multivibrator cut off valve V_4 and as a result the voltage at the anode was brought to ground. At the same time valve V_3,

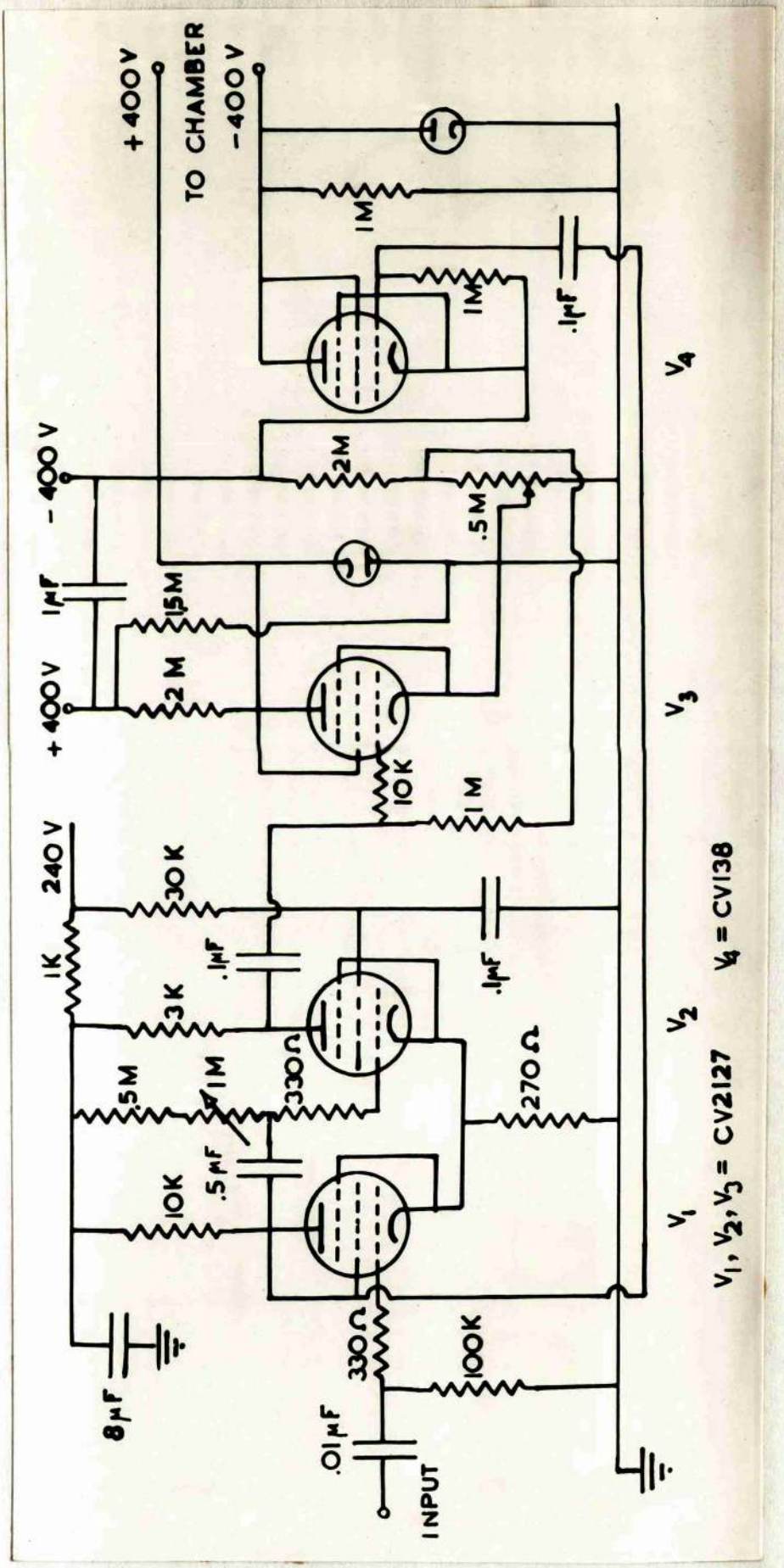

Figure 2. Circuit diagram of the clearing field switch.

which was normally cut off, was made conducting, causing a drop of +400V. across the anode resistor. The cathode of V_3 was put at a potential of -100V. with respect to ground in order that, when the valve was conducting, the anode voltage could be brought exactly to ground. It was found that the clearing voltages had to be kept off for about 20 m.sec. after the beam pulse, if no dragging of ions was to be observed.

The expansion system was operated by means of a spark valve, similar to one invented by Meyer and Stodiek (39). The pressures - in the chamber (p_1), below the rubber diaphragm (p_2) and at the spark gap (p_3) were such that the atmospheric pressure on the underface sealed the aluminium plate against two concentric O-rings; the rubber diaphragm was then in its upper position. The discharge of a 50μF condenser, charged to 2.5kV., through the spark gap disturbed the precarious pressure balance and the aluminium plate blew off with great violence. The pressures p_1 and p_2 were set automatically. A contact in a mercury manometer reading the pressure p_2 was used to operate an electromagnetic valve in an air pressure line. A

similar manometer contact operated a second valve on a vacuum line and this set p_3. By adjusting these manometer contacts the state of balance of the aluminium disc could be made very sensitive.

The speed of the valve disc was measured in a simple way. A well collimated beam of light was directed horizontally below the disc and thrown on the photo-cathode of a photo-electric valve. When the spark was discharged, the disc, flying down, cut off the beam light, and this resulted in a positive pulse at the anode of the photovalve. The pulse was led to an oscilloscope, the time base of which was triggered by the same pulse which triggered the spark. The speed of the complete opening of the valve was found to be about 3 m.sec. With this speed and 1.5 atm. of nitrogen in the chamber, the width of fast proton tracks as measured from the photographs, was about 0.5mm. The speed of the expansion of the gas in the chamber was probably of the same value, since all gas outlets were kept generously big and the rubber diaphragm was only 1/24" thick and could not cause any appreciable retardation.

The illumination of the chamber had to be very strong and uniform since the tracks were photographed with an extremely short time delay (about 23 m.sec.), after the expansion, and very fast proton tracks had to be photographed. It was only with such short time delays that one could clearly see events in the core of the high intensity γ-ray beam. On the other hand, the counter telescopes had to be placed as close as possible to the sides of the chamber and without any improper absorber in front of them. For this reason, an illuminating system with mirrors, as seen in Figure 1, was adopted. Mullard LSD16 Xenon flash lamps were employed and were operated at voltages of 1.5 atm.

Stereoscopic photographs were taken using three cameras and 5G91 film.

Since the synchrotron time is very expensive and scarce, any time unnecessarily spent on testing the apparatus at the synchrotron represents a serious waste. It is therefore of great importance, especially with an elaborate experimental apparatus as used in this experiment, to have an independent means of testing the performance of the complete experimental

set-up, under working conditions similar to those at the synchrotron, but independently of it. A triggered chamber can be tested with cosmic rays. However, this method requires considerable time and a special geometry of the chamber and counters. It was considered to be more suitable to use a miniature accelerator. A 200 kV. medical X-ray unit was available in the laboratory and was accepted for this purpose. However, originally this unit was not able to produce an X-ray pulse shorter than one millisecond, and such a pulse is required for testing a triggered chamber. This unit had therefore to be adapted for such a task. This was done by putting a condenser, thyratron controlled into the primary side of the high voltage transformer T, as is shown in the circuit diagram in Figure 3. Pressing of the button B, or applying a positive pulse to the input, caused a quick discharge of the condenser through the tyratron and transformer primary, giving rise to a high voltage of short duration in the X-ray tube.

The short X-ray pulse so produced was passed through a crystal of a photomultiplier and the chamber. A 1 Megohm resistor was used as the load of the photo-

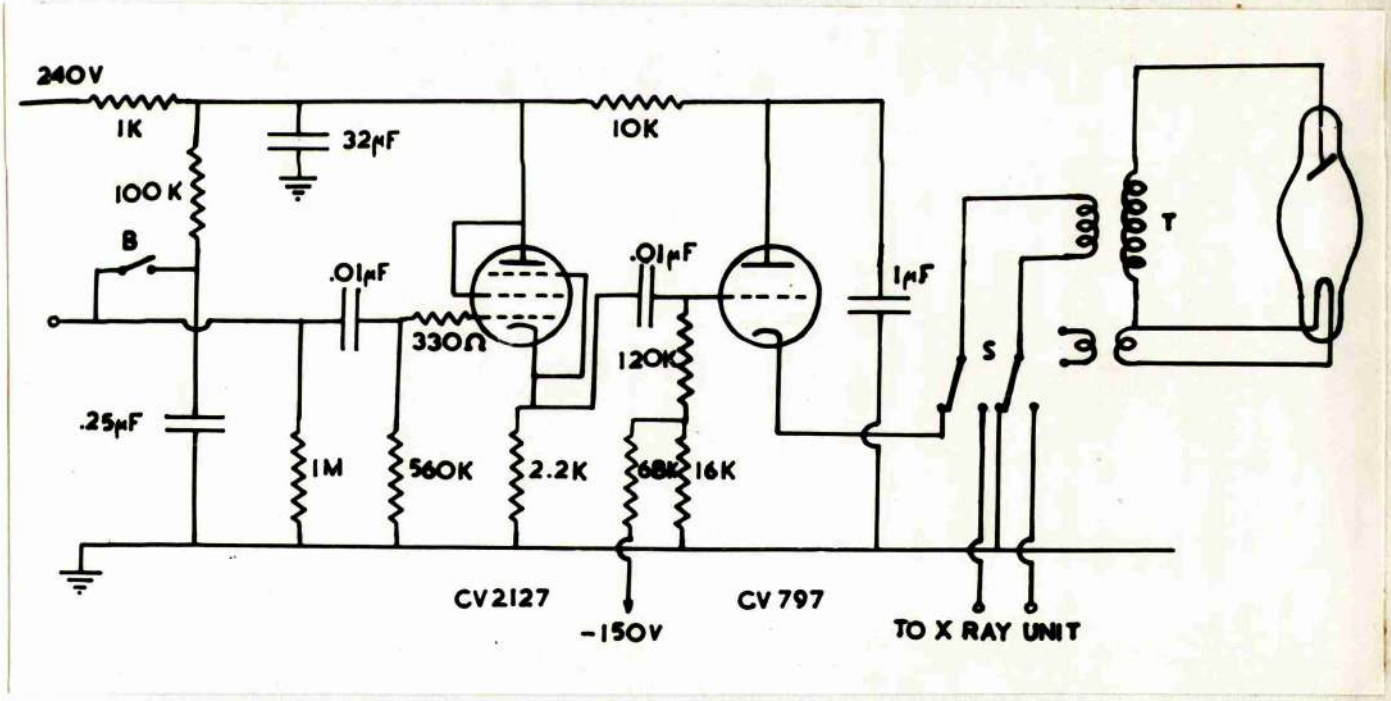

Figure 3.

Circuit for production of X-ray pulse of short duration.

multiplier collector to integrate many small pulses into a single output pulse, which triggered the chamber. In this way it was possible to check easily and quickly (a) the speed of the expansion, (b) the illumination, (c) the photography, (d) the counters and all auxiliary equipment.

2. Scintillation counter telescopes.

The technique used in this experiment to detect high energy particles involves scintillation counter telescopes, similar to those commonly used in high energy field (18, 19). However, in our case some features in the design of the telescopes and the accompanying electronics were imposed by their particular task of triggering the cloud chamber.

The telescopes were required to detect fast protons measuring their energies with an accuracy not less than $\pm$ 10 percent, and to make clear distinction between protons and other particles. In addition, it was considered that they should subtend such a solid angle that the average waiting time necessary to obtain a triggering pulse should not appreciably exceed the time of a cloud chamber cycle, i.e. three minutes. A

calculation made on the basis of cross-sections for high energy photodisintegration suggested a value for this angle of at least, 1/100 of full solid angle. In addition, an angular range from 30° to 150° with respect to the direction of the γ-ray beam was required. To satisfy these requirements, three proton telescopes, each subtending a solid angle of about 1/14 sterad. were used. They were placed at mean angles of 45, 9 and 125 degrees - (Figure 4).

Each telescope consisted of two scintillation counters set in coincidence and using plastic scintillators. The scintillators were all of the same size, viz., 10cm. x 7.5cm., and of 1.25cm. thickness. They were mounted on perspex light guides of the appropriate shape to connect them to the photo-multipliers. A good optical contact at joints was achieved by firmly pressing the scintillators by means of tightening screws and springs. Thin aluminium foil was used as a light reflector around the scintillators and light guides. EMI 6262 photomultipliers were employed in all counters. Because of the very confined space available around the cloud chamber, the external

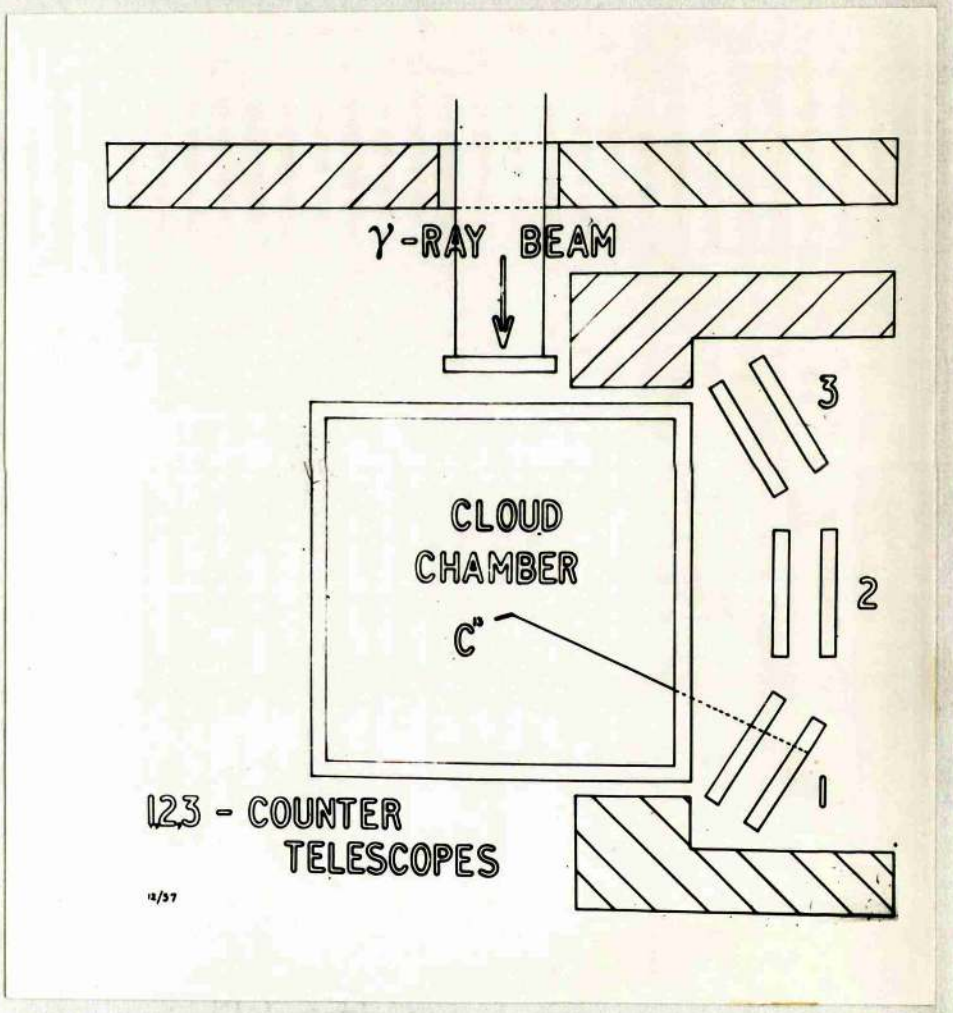

Figure 4.

Experimental layout of the cloud chamber.

dimensions of the counters were reduced to a minimum. The two scintillators of a telescope were separated by a distance of 5 mm.,and a copper absorber 1/16" thick was inserted between them. This prevented low energy electrons from producing coincidences. The photo-multipliers were operated into low (10 kohm.) impedance in order to eliminate pile-up of pulses.

The block diagram of the electronics of one telescope is shown in figure 5. Pulses from each counter, after being amplified in fast IDL amplifiers, were selected in integral discriminators and then sent to coincident circuits of 0.3 sec. resolving time. The outputs of the coincidence circuits of all three telescopes were connected to a common circuit. In this way, the unnecessary triplication of the circuits was avoided. The output of this circuit was gated by a pulse coincident with the synchrotron beam, in order to eliminate coincident pulses produced by cosmic rays. Finally, the pulses were given proper amplitude and shape by means of a Schmitt trigger circuit and sent to the cloud chamber triggering circuit.

Records were made of counts from the common out-

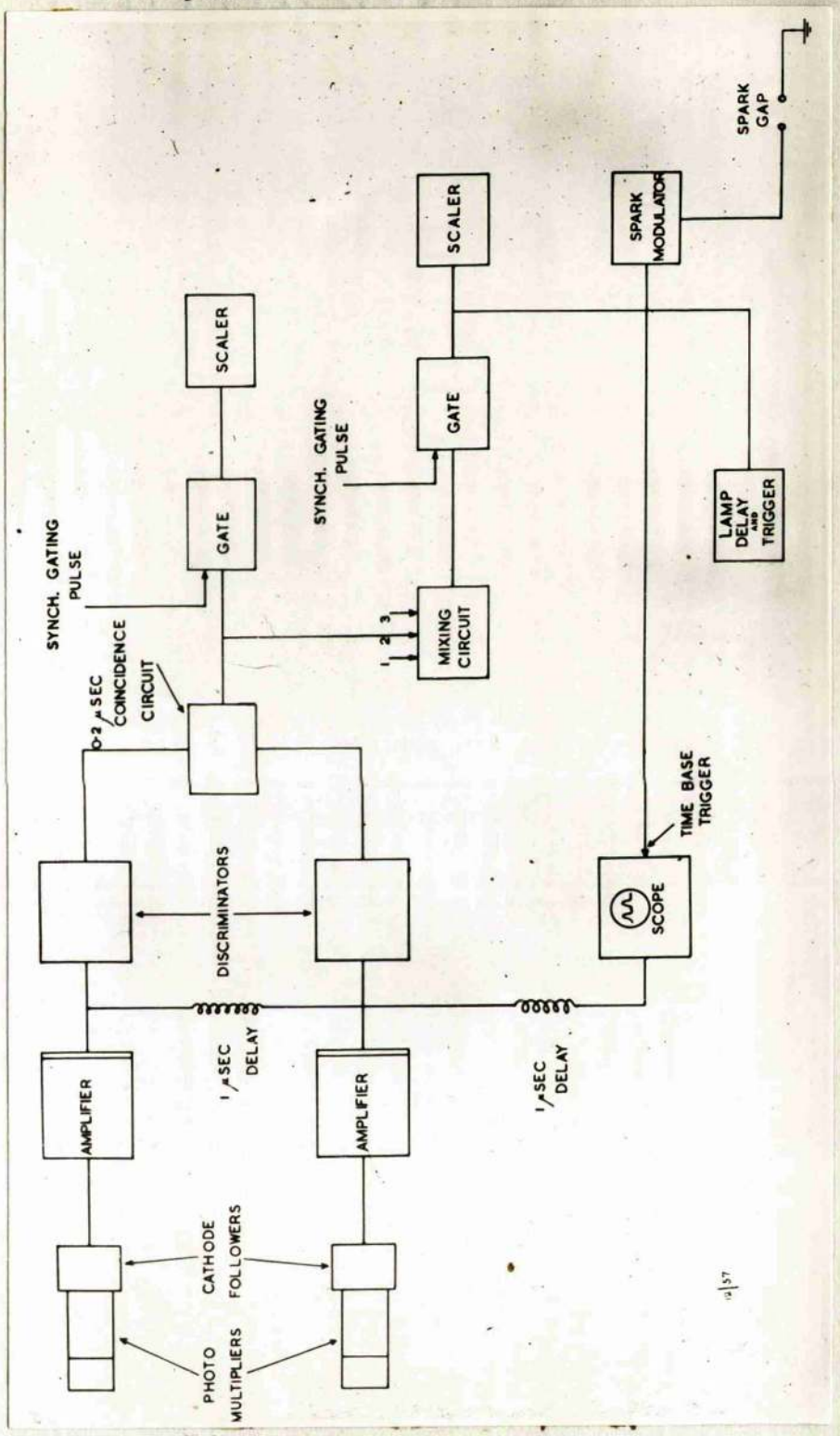

Figure 5.

Block diagram of the counter telescope electronic equipment.

put as well as from each telescope separately. In the analysis of the photographs a knowledge of which telescope triggered the chamber facilitated the finding, and at the same time, reduced the chance of misidentifying the triggering particle.

A provision was made to cut off the synchrotron beam as soon as the triggering particle.is produced, in order to reduce the beam intensity in the chamber. For that purpose a pulse was sent to the synchrotron control circuit and it caused the electron beam to be swept away from the synchrotron target.

Figure 6 shows some details of the electronic circuits. The simplest possible solutions for various circuits were accepted in order to reduce the number of components in the apparatus, already very extensive because of the need for three telescopes. Thus the coincidence circuit involves only one valve, CV2209, the screen grid of which is so constructed that it can be used as second control grid. The pulses from two counters were led to these two grids, and only when both of them simultaneously received positive pulses a negative pulse appeared at the anode. The same valve was used for the gating circuits.

In the experiment with neon in the chamber, pulses

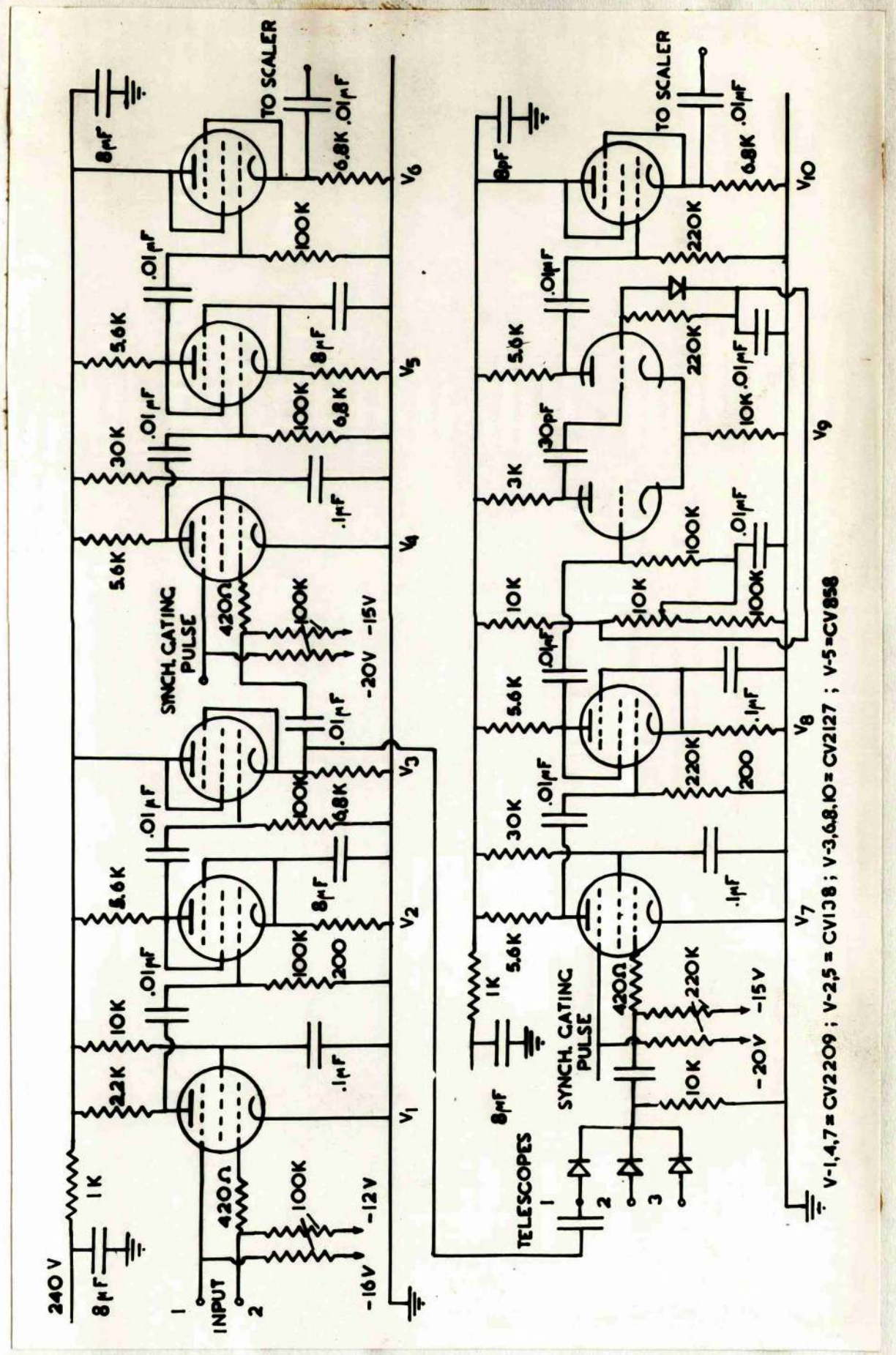

Figure 6. Coincident unit, gating and output circuits.

from the amplifiers were also displayed on a fast oscilloscope (Tektronix 210), the time base of which was triggered by the pulse from the coincidence unit. The pulses from the front counters were delayed 1 microsecond by means of a 1,000 Ohm. cable, and then further delayed, 1 microsecond together with pulses from the back counters. These pulses were photographed and later measured for every coincident count. It will be described below how these pulses were used to distinguish between protons and mesons and to determine their energies.

3. Pulse height - $\propto$ -energy calibration of the telescopes.

One of the serious problems in detection of particles with scintillation counters is the calibration of pulses in terms of particle energy losses. This problem is particularly stressed when plastic scintillators are employed, due to their non-linearity for particles other than electrons. The properties of plastic scintillators have not been fully investigated yet, and the calculated curve of light pulse $\propto$ energy is not very reliable. Nevertheless, such a curve is very useful as a preliminary guide. According to Birks (40) the specific light output of an organic scintillator is

the following function of the specific energy loss dE/dx :

$$dS/dx = \frac{A\ dE/dx}{1 + B\ dE/dx} \qquad .....(1)$$

where B is a constant. For electrons dE/dx 1 and light pulses are proportional to the energy loss in the crystal. It is not so for heavier particles because of much bigger values of dE/dx. The factor B, which indicates the non-linearity, was measured by Boreli and Grimeland (41) and was found to be 10.5 gr/Mev cm.^{2}. This value was used to calculate, from eqn. (1) the curve $dS/dx \propto dE/dx$ (Figure 7). By comparing this curve with values of dE/dx for different energies of protons and mesons, it can be seen that the light pulses are not linearly proportional to energy losses in the energy range we were interested in.

The curve from Figure 7 was used to calculate, by means of numerical integration, the total light pulse produced by protons and mesons originating in the cloud chamber gas. It was taken into account that the particles had to penetrate through the chamber wall ($\frac{1}{2}$" by Al.), and illuminating mirror ($\frac{1}{8}$" of glass) before they reached the telescope. The pulses were calculated as a function of the initial particle energy for two different thick-

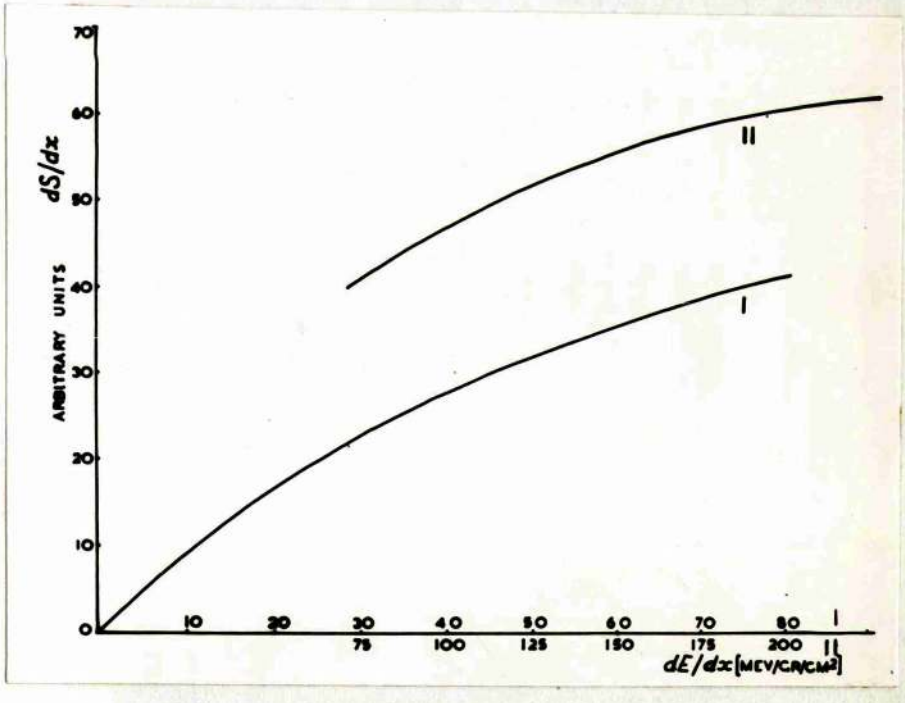

Figure 7.

$dS/dx \sim dE/dx$ for plastic scintillator.

nesses of scintillators. Range-energy data were taken from the CIT tables calculated by Aaron et al. (42). Figure 11 shows the total pulses for 1.25 cm. thick scintillators, with a 1/16" absorber between them. Curves marked A give pulses produced by protons in the front crystal, curves marked B - in the back one. Curves C and D refer to mesons. The pulses produced in the front counter represent a measure of dE/dx, and therefore are used to identify the type of particle. The pulses from the back counter determine particle energies. It can be seen from the curves that in spite of non-linearity there is still a definite difference in pulses corresponding to protons and mesons. For particles which do not stop in the back counter the pulses become less dependent on the initial particle energy. This sets a limit to the upper value of the particle energy for which a good accuracy in energy measurement can be obtained. The lowest value of the particle energy is determined by : (a) the amount of absorber in front of the telescope, in our case the chamber wall, (b) the thickness of the scintillators and the absorber between them, and (c) the required size of the pulse from the back counter.

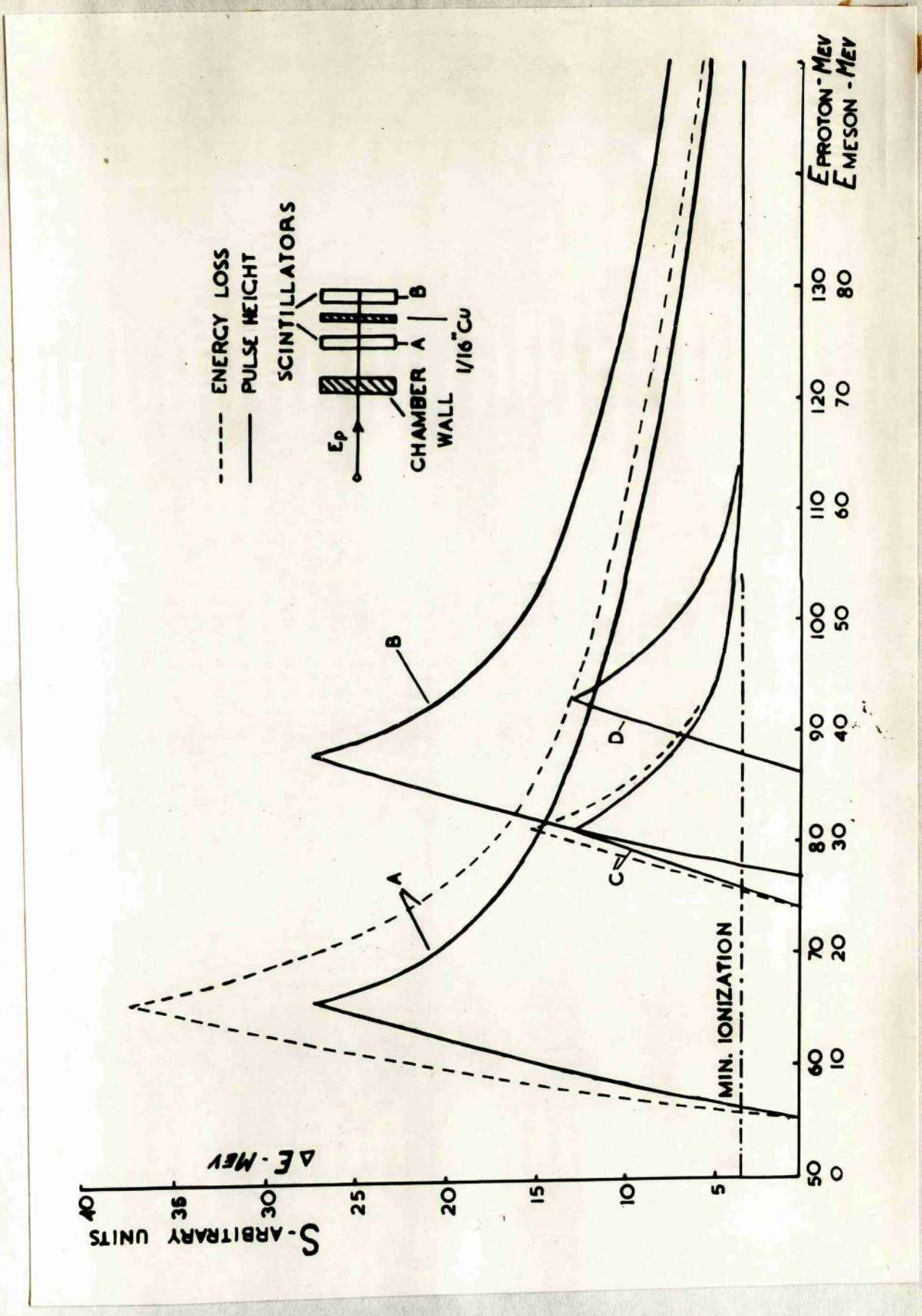

Figure 8. Total light pulses produced in the front and back scintillator.

In actual experiments two different methods were employed to determine proton energies. In experiments with helium and nitrogen the discriminator biases of front counters were set above the value which corresponds to mesons, so that only protons were detected. The back counters were biased in such a way that only those protons which nearly stopped in the crystal were accepted. However, due to the very small cross-section for the production of high energy protons, it was in practice necessary to have the proton energy spread as big as 50 Mev to get a reasonable number of counts and hence photographs per hour.

Later, in the experiment with neon, a more elaborate method of photographing pulses from both front and back counters on the oscilloscope, as described earlier was used. In this way, the particle energy was known more accurately without restricting the accepted energy spread to smaller values. With scintillators 1.25cm. thick, protons were detected in an energy range from 80 to 140 Mev, and their energies were determined within about $\pm$10 Mev.

The absolute calibration of pulse heights in terms of energy loss in the crystals of the counter telescope

was achieved by taking measurements of:-

(1) Co^{60} source Compton electron peak at about 1Mev.

(2) Th^{210} source Compton electron peak at about 2Mev.

(3) Minimum ionizing particles.

Cosmic rays were used to get the pulse size of minimum ionizing particles. Back and front counters were set in horizontal position, one above the other, at a distance of 30 cm., with 20 cm, of lead absorber between them. The scope photographs of coincident pulses were then taken. The pulses produced in the upper counter were considered to be due to minimum ionizing particles. The pulses were also measured with the positions of the counters reversed in order to calibrate both counters.

4. Sources of background.

A preliminary experiment using the synchrotron beam was performed with the purpose of checking the performance of the counter telescopes and measuring the background. A brass tube, closed at both ends with .001" thick mylar windows, was put in the beam instead of the cloud chamber, and the telescopes were placed as indicated in Figure 4. Measurements of coincidences, as well as single counting rates, were

were made with the tube filled with air and also evacuated. In this latter case the counts represented the background coming from outside the tube and from the windows, which were equivalent to about 2.5 cm. of air. For counter biases corresponding to protons the ratio of number of counts with the air in to that when a vacuum was present was found to be about 20:1. For lower biases this ratio was slowly decreasing. Thus, the background coming from outside the tube was found to be satisfactorily low.

However, the background originating in the tube itself still remained to be determined and this could not be done experimentally. The following estimation was made of the probability that particles other than protons could produce coincidences when the biases were set to such values that only protons should be detected.

(1) Mesons. Normally, pulses due to mesons should be distinctively smaller from those due to protons. However, π^- mesons are easily absorbed in nuclear matter, giving rise to stars which contain high energy protons and other heavier fragments. These particles can produce any size of pulses in counters 1 and 2

when a π^- meson is absorbed in the material in front of the telescope or in the scintillators. Although the mean free path of pions in matter is known, it is almost impossible to judge the possibility that definite pulses will be produced in the pair of counters. However, on the basis of results obtained in similar experiments, using telescopes with several counters and stricter distinction of various particles (21, 43), it was estimated that this effect could not be higher than 10 percent of the total coincident counting rate.

μ^+ Mesons, which result from π^+ decay could also produce large pulses in the first or second scintillator by virtue of their subsequent decay into an electron and neutrino. The electron can have a long path through the scintillator and thus produce a large pulse. However, the average decay time is about 2 microseconds, and could be easily resolved by the electronic apparatus employed.

π° were not considered to have any appreciable chance of producing a large coincident pulse.

(2) Neutrons. The efficiency of the telescopes for detection of high energy neutrons by way of their

scattering on protons can be approximately calculated, since the n-p scattering cross-section is known. Such evaluation gives an efficiency of less than 0.2 percent. This should be negligible, but the actual number of counts, relative to protons, could be several times higher, since neutrons of much smaller energy than protons could be detected. For example, if one sets the telescope to detect protons between 100 and 150 Mev, neutrons of energies as low as 30 Mev could give rise to pulses of the same size as protons. Taking into account that the number of fast nucleons produced by the bremsstrahlung spectrum decreases at least as the square of their energy, neutrons could be considered to contribute up to 1 percent to the counting rate. A small effect might also come from reactions produced by neutrons in the carbon content of the scintillators.

(3) "Pile-up". The γ-ray beam, passing through the experimental room and the target, produces many small pulses in each crystal, which can pile-up into larger pulses. To reduce this effect, to a negligible value, a good resolving time was required from the electronic apparatus. In our case, the length of the pulses from the photomultiplier was about 3.10^{-8} sec., and it was

and it was in amplifiers, where pulses were prolonged to about 10^{-7} sec., and in the discriminators, that the problem of piling-up could be serious. However, this source of background was made small by employing a long (about 600 microseconds) γ-ray beam. The single counting rate in each counter with low biases was of the order of 1 per 10 machine pulses. With an overall resolving time of 0.3 microsecond the piling up to large pulses could produce only a very few coincidences. This conclusion was supported by the scope photographs of the pulses from counters, which did not show any appreciable amount of piling.

The number of random coincidences was also negligible, which was verified by connecting in coincidence counters of different telescopes.

(4) Triggering protons originating at the chamber WINDOWS up to 4 cm., were not included in the results, since the illumination and photography at these regions were not sufficiently good. Because of this about 20 percent of photographs had no useful events. In the experiment with helium, where tracks were much thinner and more difficult to observe, this type of "background" amounted even to 40 percent.

The preliminary experiment with the counter telescopes also provided important information about the counter biases with regard to proton detection. This data was obtained by following a procedure described by Odian et al. (20). Thus the number of coincident counts was measured firstly, as a function of the bias of the back counter, with the bias of the front counter set just above the value corresponding to minimum ionization. The value of the back bias for which the counting rate dropped to zero corresponded to a proton energy at the maximum of curve B, Figure 8. Then the bias of the back counter was held constant, and that of the front counter varied. In this way, a region ("a plateau") was found where the counting rate did not depend on the bias of the front counter. Later, in the experiment itself, this bias was set comewhere in the middle of this plateau.

5. Experimental lay-out and procedure of measurement.

All of the investigations in this experiment were performed using, as a photon source, the bremsstrahlung beam from the Glasgow 300 Mev synchrotron. The γ-ray collimator system used at this synchrotron was described by Atkinson et al. (44), and is shown in Figure 9.

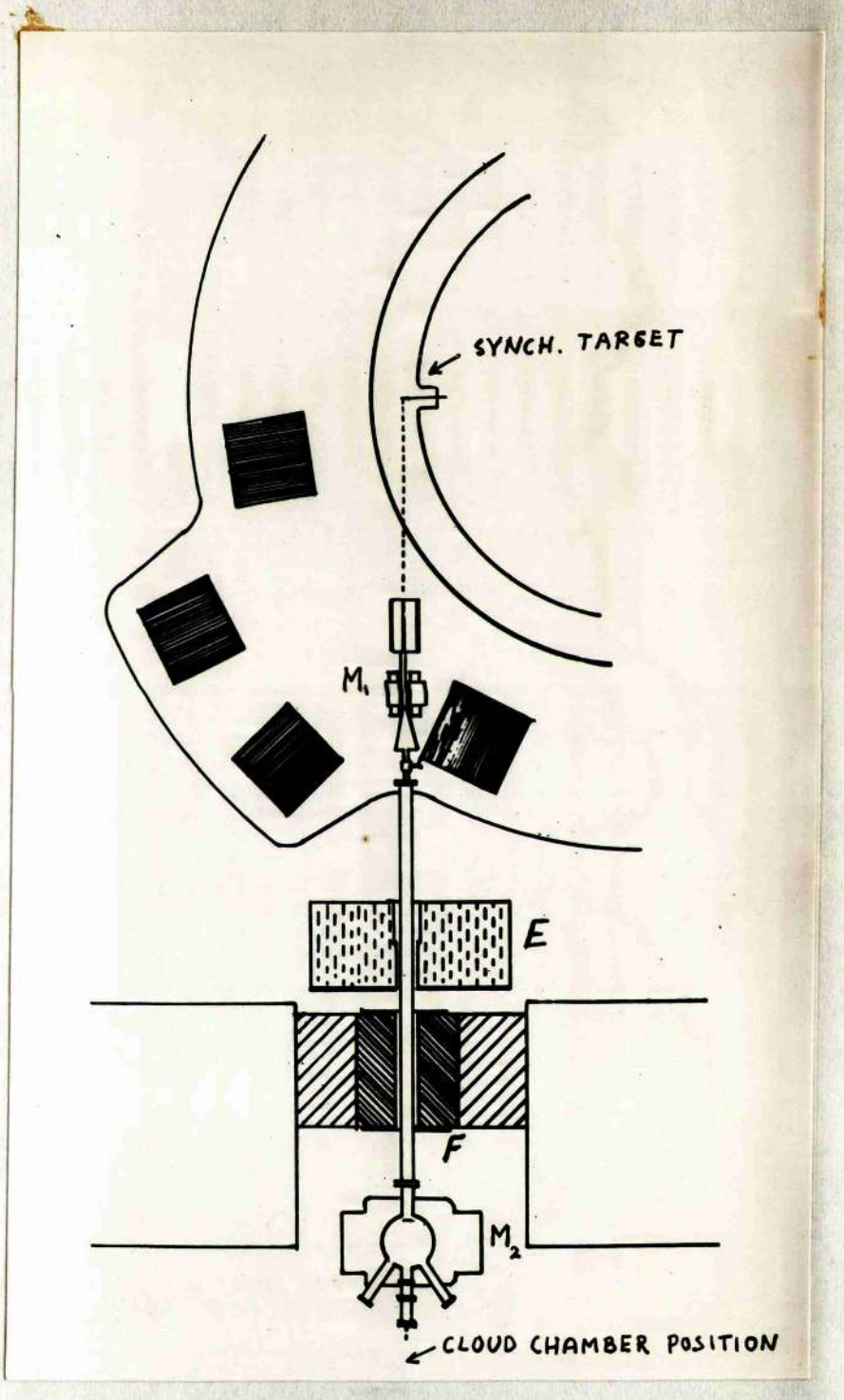

Figure 9.

γ-ray beam Collimator system.

The γ-ray beam was collimated by a water tank (E), and a lead shield (F). The angular divergence of the beam at a distance of 6 meters from the synchrotron target, where the chamber was placed, was .2 degrees , and its diameter was approximately 2 cm. Two magnets were used to clean the beam from electrons. Firstly, a scrubbing magnetic field deflected charged secondary particles out of the beam. Then, after leaving the collimator, the gamma-rays passed once more through another magnetic field of 5,500 gauss, produced by a pair specrrometer. This field deflected out of the beam secondary elecrons created by the γ -rays in striking the window at the front of the collimator and the channel walls. With this collimating system, the γ -ray beam, as obtained in the experimental room,was clean and well defined.

In our experiments with the chamber an additional step was taken to reduce the core of secondary electrons produced in the chamber itself. A rod of light plastic material (perspex), 30 cm. long and 3 cm. in diameter, was placed in the γ-ray beam before it entered the scrubbing magnet. This absorbing material, in virtue of its relatively higher absorption for low energy

gamma rays, reduced the low energy part of the bremsstrahlung spectrum which was mostly responsible for the chamber background, leaving the high energy part little changed in intensity.

The general lay-out of the experimental apparatus is shown in Figure 4. The chamber was placed behind an iron shield, at the end of the evacuated beam tube. Great care was taken to see that the beam in passing through the chamber, would not touch the metal frames of the windows. After the alignment was done optically, the correct position of the chamber was verified by exposing X-ray plates at the entry and exit windows.

The electronic apparatus was switched on several hours before each experimental run, in order to enable it to reach a steady temperature before the beginning of the experiment. The same was done with the cloud chamber, and the whole apparatus was thoroughly checked and adjusted. The expansion ratio of the chamber was set at the highest possible value; this step was found to result in better quality of tracks, probably because of more vapour being available in the highly ionized gas.

The γ-ray intensity was monitored with an ionization chamber identical to one calibrated and used at Cornell. It is estimated that this type of monitor is inaccurate by about ± 5 percent.

The telescopes were checked with radioactive sources from time to time in the course of experiments, and their positions were often interchanged, so that on an average, each telescope occupied one position for one third of the total running time.

The films from the cameras were alternately developed, without a halt in the experiment; to control regularly the quality of the photographs.

The following sequence of events was involved in taking one photograph:

(1) Chamber ready for expansion.

(2) Lights in the beam room switched off; the shutters of the chamber and scope cameras opened.

(3) Synchrotron pulsing started.

(4) A telescope triggered the chamber.

(5) Illumination and photography.

(6) Chamber and scope camera shutters closed, film wound on.

(7) Chamber re-set and the slow clearing expansions

applied.

(8) Records made of - (a) the telescope which triggered the chamber, (b) γ-ray integrator reading, and average intensity of the beam, and (c) the time interval of the irradiation.

(9) Chamber ready for next expansion.

The frames on the chamber and scope films were marked in order to correlate them easily in the later analysis of photographs.

The pressure in the chamber was determined by its design, and it could not be lower than 110 cm. However, with nitrogen or neon at this pressure in the chamber, the expected recoil ranges would be too short for an accurate measurement. The chamber was therefore filled with a mixture of 60 cm. of nitrogen and 50 cm. of helium. It was estimated that helium events would constitute less than 10 percent of the total number of events, and, in addition, they should be easily recognizable. With this gas mixture in the chamber, the stopping power of the gas was reduced by 30 percent, this being equivalent to 0.9 atmosphere of air, and the beam core in the chamber was lighter. In the experiment with neon the gas mixture consisted of 80 cm.

of neon, and 30 cm. of helium and was equivalent to 0.72 atmosphere of air, but since the chamber could not be evacuated completely some 2-3 percent of nitrogen was present, in addition to alcohol and water vapour. The experiment with helium was done with pure helium in the chamber, but again alcohol and water vapour as well as 5.2 percent of nitrogen were present.

6. Analysis of photographs.

Stereoscopic pictures of the tracks in the cloud chamber were taken with three cameras. After the film was processed the images were reprojected through the same optical system. A white movable plate, which could rotate round the middle line, was placed in the position of the chamber, its axis of rotation being directed along the gamma ray beam. The plate was first put in a position corresponding to the bottom grid of the clearing field wires, and the positions of the cameras adjusted until three images of the grid coincided. This was later checked for each photograph. The next step was to move the plate vertically until the origins of images of an event coincided. The plate was then rotated around its axis and the true positions of each track of the observed event found. Two angles were measured for each track: (1) the angle of the tilt of the plate, (2) the angle of the track with respect

to the γ-ray beam direction (measured in the plane of the two). In addition, the range of those tracks which stop in the chamber gas was measured, and the relative track densities and the positions in the chamber noted. The angles of tracks longer than several millimeters were measured with an accuracy of $\pm$ 1 degree, and the track lengths were estimated to 0.3 mm. The true length of a recoil was taken to be the total length of the track less the width of the track. Recoils were measured down to length of 1 mm.

The criterion for a track to be accepted as being due to the triggering particle was:-

(1) To agree with the record referring to which telescope had caused the triggering.

(2) To be within the solid angle subtended by the corresponding telescope.

(3) To have appearance of a high-energy proton track, that is, to be very thin and straight.

With these conditions, it is felt that no "wrong" tracks whatever, have been accepted as the genuine ones.

CHAPTER III.

EXPERIMENTAL RESULTS.

1. Helium.

The experiment with helium in the cloud chamber proved to be very difficult because; (a) helium is a mon-atomic gas, with very low cross-section for high energy photodisintegration, (b) a 100 Mev proton track in helium is very difficult to observe and to photograph, and (c) the triggered cloud chamber requires the use of alcohol and water vapour mixture, thus heavier gases than helium must be present. Despite these difficulties, it was considered worth while to attempt such an experiment for two reasons.

Firstly, at the time there were no experimental data on the high energy photodisintegration of helium. Secondly, an appreciable proportion of helium was present in the chamber in the experiments on neon and nitrogen. Therefore, it was considered useful to have evidence of the type of events coming from helium, in order to eliminate them from the results.

Regarding the first point, it should be mentioned that only three reactions leading to the emission of high energy protons exist in helium (meson processes

excluded):-

(1) He^4 (γ ,p)H^3 , Threshold 19.8 Mev.

(2) He^4 (γ ,pn)H^2 , Threshold 26.1 Mev.

(3) He^4 (γ ,p2n)H , Threshold 28.4 Mev.

The cloud chamber is able to distinguish the reaction (1) from reactions (2) and (3), the proton and triton in (1) being coplanar with the γ-ray. (2) and (3) can not be separated without a magnetic field.

The reaction (1) is very suitable as a check of counter telescopes, since proton energy is defined by the proton and triton angles of emission with respect to the γ-ray beam. Hence the spread in proton energy can be measured independently from the telescopes, and also the counter pulses calibrated. Unfortunately, this reaction appeared to be much less probable than (2) and (3).

About 220 good photographs were taken in the experiment on helium, and 57 events associated with the emission of high energy triggering protons were identified. Table 1 shows these events divided into groups according to the number of prongs.

TABLE I.

EVENTS OBSERVED IN HELIUM.

1 prong	2 prong coplanar	2 prong non-coplanar	3 prong	4 prong	5 prong	Total
2	4	28	7	11	5	57

Since no reaction leading to three or more prongs, meson production excluded, exists in helium, such events were taken as due to carbon and oxygen from alcohol and water vapour, and to nitrogen. This latter was present in 5.2 percent* since the chamber could not be evacuated completely and was filled by a repeated procedure of filling and evacuating it. In most of these events one or more very heavy fragments were present which could not originate in helium. In none of these cases, was it possible to fit an event as a meson produced in helium.

Also those events from the third group (2 prong non-coplanar) in which the recoil was very heavy and of short range were considered to be due to C, O or N.

Alcohol and water vapour pressures were calculated by using Raoult's Law. These pressures were:

* This was later found by mass spectrometer analysis of the gas sample.

alcohol :2.2cm. water :0.9 cm.

The events due to helium after this subtraction were:

(1) 2 prong coplanar: 4

(2) 2 prong non-coplanar: 24.

For events in the group (1) the momentum and energy balance was calculated and three of them fitted as the reaction $He^4(\gamma, p)H^3$.

The relevant data are presented in Table 2 where E_p, E_T, Θ_p and Θ_T denote the energies and angles of proton and triton respectively.

TABLE 2

E_γ Mev	E_p Mev	E_T Mev	Θ_p	Θ_T
135	89	26	63	98.5
152	100	33	85.5	74.5
173	113	37	77.5	81.5

One event from this group could not be fitted in this way.

Events in group (2) were interpreted as the reactions (3) or (2). In only two cases did the recoiling particle (proton or deuteron) stop in the chamber gas, so that the neutron angle and energy could be calculated

(Table 3), where: Θ_{ND} is the angle of neutron in the photodisintegration of deuterium, corresponding to the proton energy and angle, given in the table. The recoil particle was taken to be deuteron.

TABLE 3.

E_γ Mev	E_p Mev	E_D Mev	E_N Mev	Θ_P	Θ_N	Θ_{ND}
243	80	1.2	136	96	72	63
175	80	1.1	67	87	71	75

In other cases the recoil did not stop, but from the appearance of the tracks these events could be classified in three categories:

(1) Low energy recoil of range > 4 cm. - 4 events.

(2) Medium energy, range > 12 cm. ($E_D > 2$ Mev) - 13 events.

(3) High energy recoil (if proton $E_p > 20$ Mev) - 5 events.

In eight of these cases the angle between the triggering proton and the recoil particle was such that it was obvious that a high energy neutron was also emitted. Events in group (3) showed a correlation in the directions of the two charged particles: the angle between them was always bigger than 125° and they were not far

from coplanarity (within 10°). Hence the coplanar event which did not fit as the $He^{4}(\gamma, p)T$ reaction could be of this type.

This cross-section, calculated for the production of protons going into the forward telesoope (angle of 67 $\pm$ 13 degrees), was found to be:

$$\sigma = 0.7.\ 10^{-31} cm^{2}/Mev\ Q\ sterad.$$

In this cross-section 2 events of $(\gamma, p)T$ type, and 12 of (γ, pn) type are included.

The ratio of events going into front (mean angle 67°), middle (90°) and back (113°) telescope was 12 : 10 : 2.

Events in helium due to C, O and N were also analysed. Table 4 shows these events divided into subgroups:-

TABLE 4.

1 prong	2 prong non-copl.	3 prong Triggering particle plus 2heavy	3 prong Triggering particle plus 1 heavy 1 light	4 prong Triggering particle plus 3heavy	4 prong Triggering particle plus 2 heavy 1 light	4 prong Triggering particle plus 1 heavy 2 light	5 prong
2	4	3	4	7	3	1	2

In two of the four prong events all three heavy fragments stopped in the chamber gas. Assuming that they were due to the reaction $N^{14}(\gamma, pn)3\alpha$ (commonest in Nitrogen)

the calculation of the neutron and γ-ray energies gave the results presented in Table 5.

TABLE 5.

E_γ Mev	E_p Mev	E_N Mev	$E_{3\alpha}$ + $E_{thresh.}$ Mev	θ_p	θ_N	θ_{ND}
175	80	72	8.7	84	70	57
128	80	17.5	16.7	107	60	50

Events in Table 4 were divided into two groups, one group being due to C and O, and the other to N. This was done on the basis of proportions of nuclei and assuming an A-dependence of cross-sections. In this way, it was possible to subtract events due to C and O from the nitrogen and neon results.

2. Nitrogen.

About 300 usable photographs with nitrogen in the chamber were taken and a total of 168 events associated with the high energy triggering proton was found and analysed. These events are presented in Table 6, where a separation is made of events due to He, C and O.

TABLE 6.

Events observed in Nitrogen.

	1 prong	2 prong	2 prong coplanar.	2 prong non. coplanar	3 prong	4 prong	5 prong	6 prong	TOTAL
N	5	3	26	38	51	13	1		137
He		1	11	-	-	-	-		12
C+O	-	-	3	2	5	2	-		12
Not identified		5	-	-	-	-	-		5
TOTAL	5	9	40	40	56	15	1		166

Events in the first column (1-prong) were probably due to the $N^{14}(\gamma, pn)C^{12}$ reaction, where the C^{12} recoil energy was very small. They will therefore be included in the third group (2-prong non-coplanar).

The momentum and energy balance for the events in the second group was calculated on the assumption that they were due to the $N^{14}(\gamma, p)C^{13}$ reaction. Three of these

events were satisfactorily fitted and had recoil energies of the expected values. Table 7 shows the relevant data for this group.

TABLE 7.

E Mev	E_P Mev	E_R Mev	P	R
98	82	4.7	43.5	125
141	120	6.0	36	131.5
144	125	6.7	43	122.5

Events in the third column were taken as due to the $N^{14}(\gamma, pn)C^{12}$ reaction. In thirteen cases the neutron energy and the angle of emission were calculated (Table 8). In other cases the recoil ranges were short and the angles could not be measured precisely.

C^{12} range-energy relations obtained by Lillie (45) were used to calculate the recoil energies.

TABLE 8.

E_γ	E_P Mev	E_N	Θ_P	Θ_N	φ_N	Θ_{ND}
129	100	4	50	128	0	93
155	100	32	100	63	9	48
170	100	48	109	62	3	40
208	100	85	90.5	77	28	61
286	100	165	96.5	68	34	50
200	100	80	85.5	72	143	62
140	100	13	70	20	11	74
277	100	151	78	61	36	62
228	100	106	134	27	13	34
170	100	49	39.5	172	73	126
147	100	21	50	54	62	105
157	100	35	59	93	27	92
166	100	41	64	61	36	90

In this table Θ_P and Θ_N denote the proton and neutron angles with respect to the γ-ray beam direction, φ_N is the neutron azimuthal angle, and Θ_{ND} is the angle in the photodisintegration of deuterium, corresponding to the given proton energy and angle.

The distribution of recoil energies for all (γ,pn)

events is given in Table 9.

TABLE 9.

Recoil energy in the interval (Mev)	0 - 1	1 - 2	2 - 3	3 - 8
Number of events	14	5	5	8

If the recoil energy comes from the internal momentum, which is equal and opposite to the quasi-deuteron momentum (Section 3, Chapter 1), then the corresponding quasi-deuteron energies are 6 times greater than the recoil energies.

A survey of 3-prong events is given in Table 10.

TABLE 10.

Triggering particle plus.		
2 heavy	1 heavy 1 light	1 heavy 1 very fast
22	8	8

In eight cases of the first group both heavy tracks were of very similar appearance. They were interpreted as the reaction $N^{14}(\gamma,pn)2Li^{6}$, since no other reaction

is possible which would split the residual C^{12} nucleus into two equal fragments. The threshold for this ($C^{12} \rightarrow 2Li^{6}$) reaction is 28 Mev. A typical event of this kind is shown in Photograph 1. Table 11 gives the calculated data for four of these events, in which both fragments were certain to terminate in the chamber gas.

TABLE 11.

E_γ	E_P MeV	E_N	$E_{2Li6} + E_{thresh.}$	Θ_P	Θ_N	φ_N	Θ_{ND}
228	100	72	43.4	78	55	0.5	65
210		59	38.5	86.5	71	47	63
210		68	35.9	89	66	56	60
170		40	47	50.5	36	38	92

The remaining 14 events in this group can be due to the reaction $N^{14}(\gamma, pn)(Be^{9} + He^{3})$, which has a threshold of 26 Mev.

The only reactions which can produce events of the type listed in the second and third column of Table 10 are those which C^{12} splits into $(B^{11} + p)$ (threshold 15.8 Mev), or $(B^{10} + D)$ (threshold 25.1 Mev).

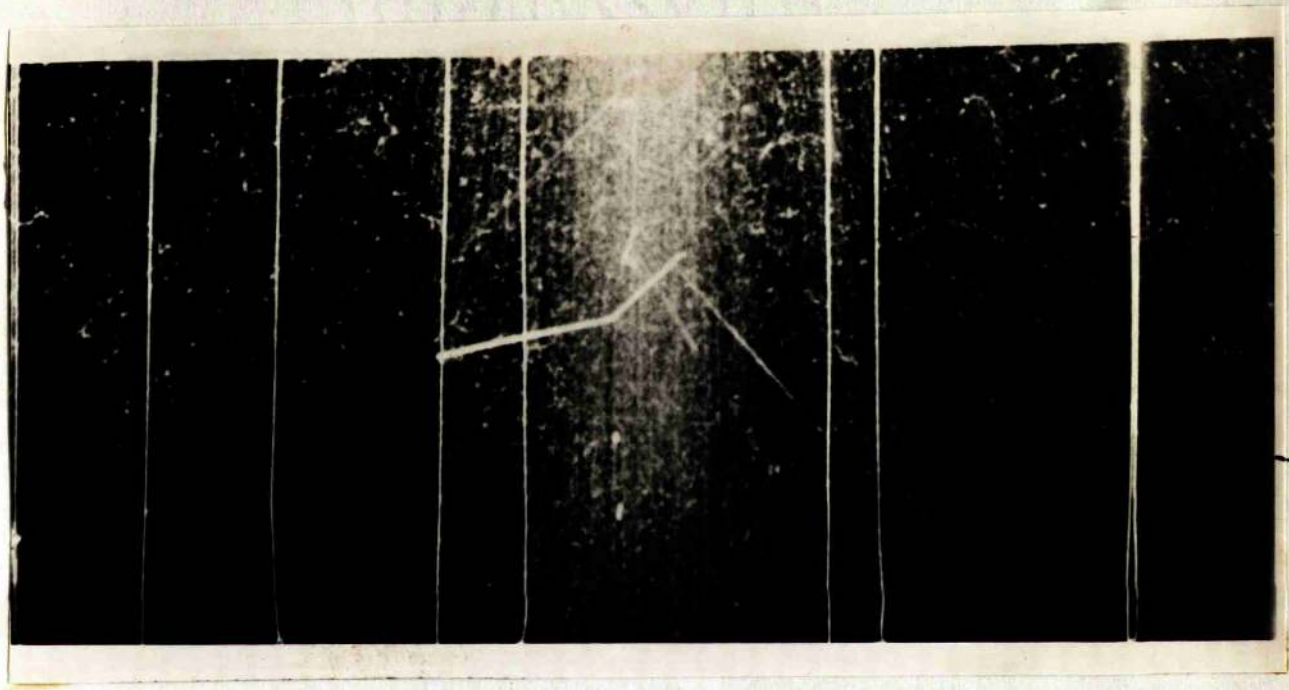

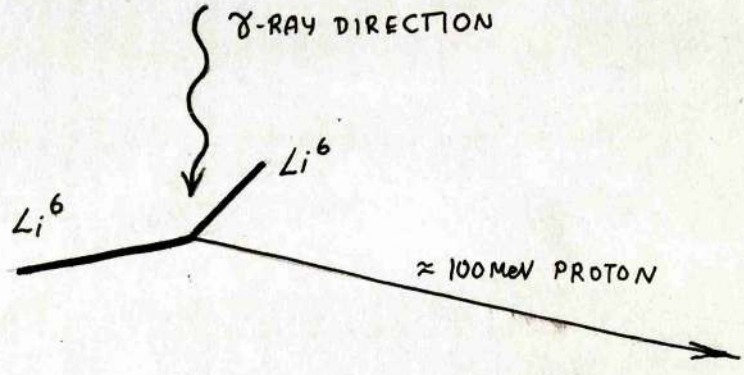

Photograph 1.

Example of the $N^{14}(\gamma, pn)2Li^{6}$

In all events in the third column the fast particle was of very high energy (if proton, $E_p > 40$ Mev) and was almost coplanar with the triggering proton.

The 4-prong events divided into subgroups are shown in Table 12.

TABLE 12.

TRIGGERING PARTICLE PLUS			
3 heavy	2 heavy 1 light	1 heavy 2 light	2 heavy 1 very fast
28	13	6	6

In almost all events in the first column all three heavy fragments were of comparable track thickness. It is very probable that they represent the $N^{14}(\gamma, pn)3\alpha$ reaction. The threshold for the $C^{12} \rightarrow 3\alpha$ reaction is 7.2 Mev. A typical event of this type is shown in Photograph 2. In seven of these cases all heavy particles terminated in the chamber gas, and all energies and angles could be calculated (Table 13). They showed two distinctive groups. In one there was

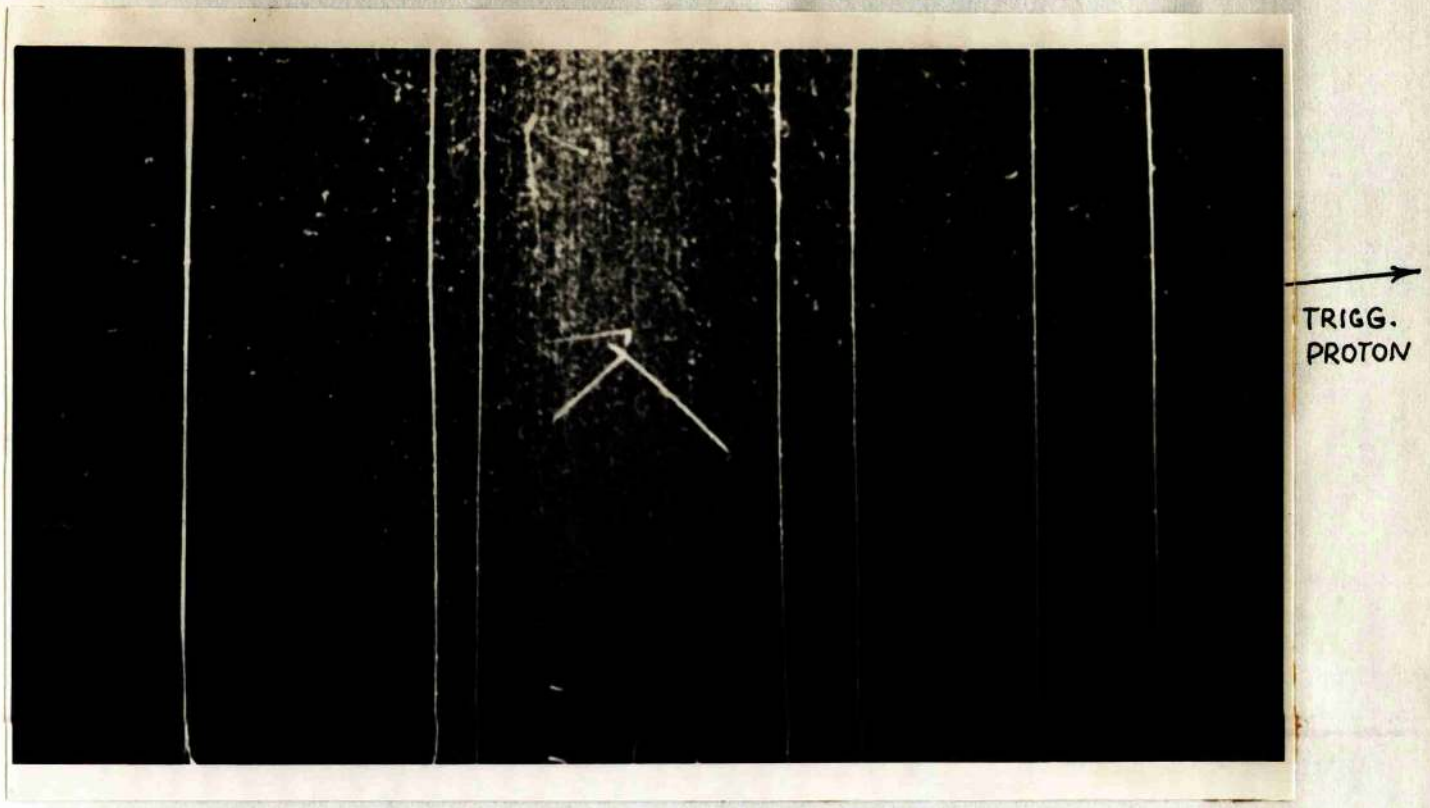

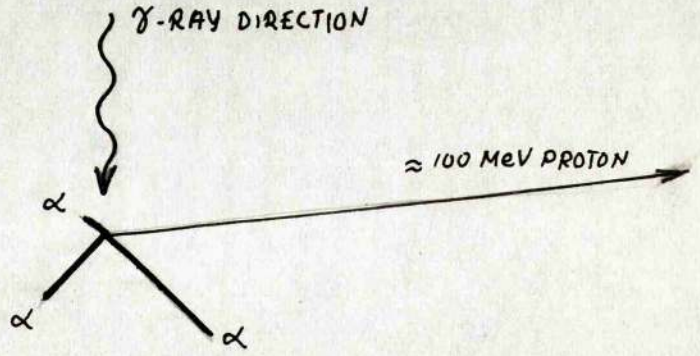

Photograph 2.

Example of the $N^{14}(\gamma, pn)3\alpha$

a high momentum.

TABLE 13.

E_γ	E_P Mev	E_N	Θ_P	Θ_N	φ_N	Θ_{ND}	$E_{3\alpha}$ + E_{thresh}
198	120	38	38	150	1	120	27.1
192	120	40	44	130	51	118	19.6
212	120	56	54	76	2	100	23.1
230	100*	103	93	84	5	48	14.4
162	120	7	45	120	5	109	15.6
157	120	1.2	64	107	11	118	22.5
130	100*	1	51	78	85	92	16.2

unbalance, indicating an emission of a high energy neutron. In the other, the unbalance was very small.

The minimum kinetic energy carried by fragments in all events from the first column[1] was estimated on the assumption that they were α-particles, and its distribution is shown in Table 14.

TABLE 14.

Minimum energy of fragments, including the threshold for $C^{12} \rightarrow 3\alpha$, --Mev	15	25	35	45
Number of events	9	12	4	3

*In these cases the assumption of E_p = 120 Mev gave E_γ > 300 Mev

1) Table 12.

The events in the columns 3 and 5 of Table 12, can be due to the following reaction, if the fast particle is taken as proton:

$$N^{14} + \gamma \rightarrow C^{12} + p + n;$$

$$C^{12} \rightarrow Li^{7} + He^{4} + p$$

The threshold for the latter process is 28 Mev. The only other probable process would be one in which Li^{7} would, additionally, split into $Li^{6} + n$.

The fast particles in the last column of Table 12 were nearly coplanar with the triggering particle, and their angles of emission were roughly equal to the angle which would occur in a two body (p-p) photodisintegration.

The events with 5 or 6 prongs could not be identified as particular reactions. The minimum energy required to produce an event of these numbers of prongs is about 40 Mev. A rough estimation of the minimum kinetic energies of fragments in these events showed that only in 3 events was this energy below 20 Mev. In four of these events a very fast particle was among the fragments, and in one case it was almost in the same plane as the triggering proton.

The cross-section for the photoproduction of protons of mean energy of 100 Mev at an angle of 52 $\pm$ 12^{o} was found to be:

$$6 = 0.4.\ 10^{-30} \text{cm}^2/\text{sterad MevQ}.$$

Finally, in the events marked "not identified" in Table 6, which were coplanar within 2 degrees, the angles of the triggering proton and recoil with respect to the γ-ray beam were of such values that it was impossible to fit these events as (γ ,p) reactions for γ-ray energies up to 330 Mev. A low energy neutron was in each case involved, but it is hard to explain how all three particles happen to be in the same plane.

3. Neon.

For technical reasons the synchrotron energy in the experiment with neon in the cloud chamber was 240 Mev. A total of 300 good photographs was taken, and 185 events associated with the triggering particle were found. Table 15 shows the distribution of these events according to the number of prongs. The events due to carbon, oxygen and nitrogen were separated and they are also given.

TABLE 15.

Events observed in neon.

	2 prong coplanar	2 prong non-coplanar	3 prong	4 prong	5 prong	6 prong	7 prong	TOTAL
Ne	4	32	60	25	17	11	1	150
C+O+He		16	4	8	3			31
Not identified	4							4
TOTAL	8	48	64	33	20	11	1	185

Events in which only the triggering particle could be seen (1-prong) are included in the 2-prong non-coplanar group (there were five of these events).

The energy and momentum balance were calculated for the events in the first column under the assumption

that they were due to the $Ne^{20}(\gamma,p)F^{19}$ reaction (threshold 12.8 Mev). An event of this type is shown in Photograph 3.

In the case of four of these events a fit was possible (Table 16), while the remaining four, classified as "not identified", in Table 15, were of the same type as in the case of nitrogen.

Table 16.

E_γ	E_P Mev	E_R	Θ_P	Θ_R
145	128	5	52.5	111
115	96	5.8	81	84.2
130	112	5.1	67.5	96.5
123	104	5.4	65	100.5

The events in the third column correspond to the $Ne^{20}(\gamma,pn)F^{18}$ reaction (threshold 23.2 Mev). One of these events is shown in Photograph 4. The relevant data for those events of this group which had recoil ranges $>$ 4 mm is presented in Table 17. A theoretical range-energy curve for F^{18} was used. From the oscilloscope pulses in the scintillators , it was found that the proton energy in the majority of cases was

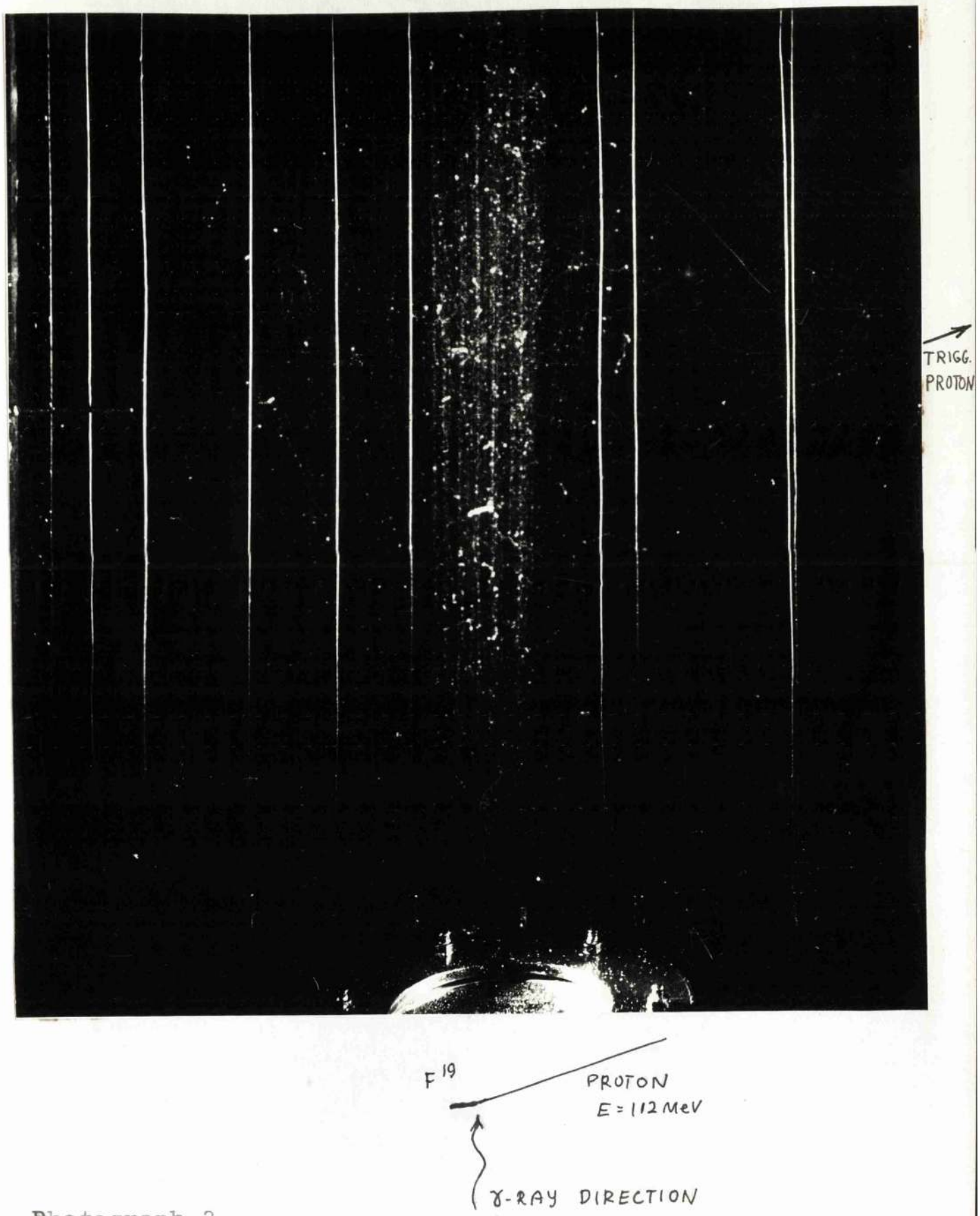

Photograph 3.

Example of the $Ne^{20}(\gamma, p)F^{19}$

between about 85 Mev and 115 Mev, and a mean value of 100 Mev was taken in the calculations.

TABLE 17.

E_γ	E_p Mev	E_N	Θ_P	Θ_N	φ_N	Θ_{ND}
173	100	48	102.5	84	37	48
208	100	83	59	78	28	92
155	100	45	59	81	46	92
201	100	76	107	39	19	76
138	100	13	115.5	70	12	40
158	100	33	90	65	18	62
182	100	57	55	160	35	94
132	100	7	60	71	14	91
138	100	13	51.5	57	30	98
174	100	49	76.5	61	32	76
221	100	96	86	46	9	62
235	100	110	83	41	19	64

In Table 18 the energy distribution of all F^{18} recoils is presented.

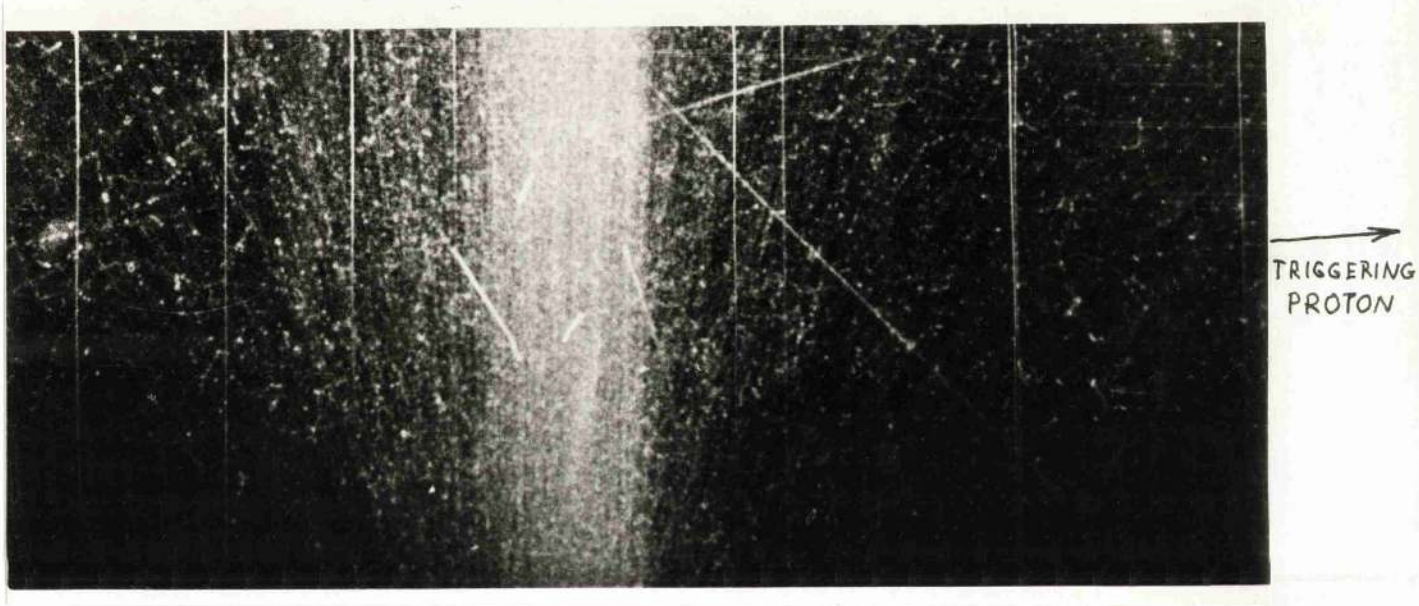

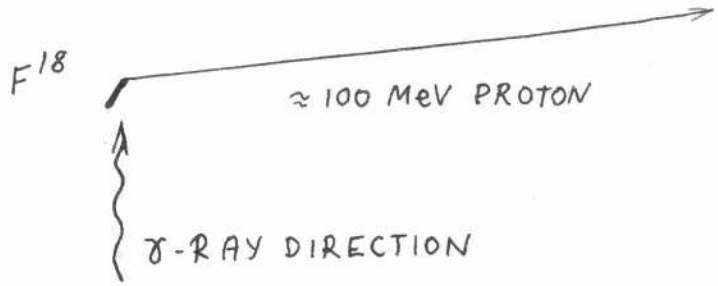

Photograph 4.

Example of the $Ne^{20}(\gamma,pn)F^{18}$

TABLE 18.

Recoil energy in the interval - Mev.	0 - 1	1 - 2	2 - 3	3 - 5
Number of events.	14	9	4	5

The events in the third column of Table 15 can be divided into three groups, according to the appearance of tracks., (Table 19). In many of these groups, it was obvious that a neutron was also emitted.

TABLE 19.

	TRIGGERING PARTICLE PLUS	
2 heavy	1 heavy 1 light	1 heavy 1 very fast
44	14	2

In the case of twelve events of the first group, both heavy fragments were of similar appearance and length. Since some of them obviously involved the emission of high-energy neutrons, it is probable that they represent reactions in which the residual nucleus F^{18} was split

into two fragments. Two such reactions are possible*:-

$$F^{18} \quad C^{12} + Li^{6} \text{ ; Threshold 13 Mev.}$$
$$F^{18} \quad C^{11} + Li^{7} \text{ ; Threshold 24.6 Mev.}$$

In other events of the first group, one of the fragments was of much longer range than the other. It is very probable that they correspond to a reaction where F^{18} splits into $N^{14} + \alpha$.

The threshold for this process (=4.4Mev) is the lowest for all possible reactions in F^{18}.

The kinetic energies of the fragments in these events were not high; mostly between 10 and 20 Mev.

In the case of other multi-prong events it is difficult it attribute them to particular reactions, since many possibilities exist. The minimum energy required to produce a 4-prong event in Neon is about 30 Mev (neutron emission not assumed) and for a 5-prong event, about 40 Mev. The kinetic energies of fragments in these events, while difficult to estimate, were certain to be rather high. There were very few 4 or 5 prong events in which the sum of the kinetic energies of fragments was not greater than 20 Mev. In the case of 8 of these events there was a very energetic particle among the fragments, and this particle was never far from

* F^{18} can also split into $B^{9} + Be^{9}$, but it is not known whether the half life of B^{9} is longer than several m.sec.

the horizontal plane (i.e. the plane of the triggering proton).

The cross-section for the photoproduction of a 100 Mev proton at an angle of $65 \pm 15^{\circ}$ from neon was found to be:-

$$\sigma_{65} = 0.4 \cdot 10^{-30} \text{cm}^2/\text{sterad Mev Q.}$$

The ratio of events in the front (mean angle 65°), middle, (90°) and back telescope, (115°) was:

78 : 54 : 18.

4. Discussion of results.

The common feature of the results of all three experiments is that high-energy neutrons are often emitted in coincidence with high-energy protons. In addition, the angle of neutron emission is roughly that in which neutron would have travelled had it been emitted in the photodisintegration of deuterium. Thus, these results are basically in accordance with the quasi-deuteron model of high energy photonuclear effect. However, the question arises as to whether multi-prong events, so common in our results, are also connected with this type of γ-ray absorption. One can suppose that these events represent those cases in which the neutron was absorbed or scattered on its way out of the nucleus. The probability of this can be calculated on the basis of the mean free path (Λ) of nucleons in nuclear matter. Thus following Serber (46) and Gottfried (38) we can write for the probability that both proton and neutron will escape from the nucleus without being absorbed:

$$f_1 = \frac{1}{V_o} \int e^{-x/\Lambda} \cdot e^{-y/\Lambda} dV_o$$

where V_o is the volume of the nucleus, and x and y are

distances travelled by the proton and neutron, respectively, from the point of their origin to the nuclear surface.

Similarly the probability that the proton will escape and the neutron will be absorbed is:

$$f_2 = \frac{1}{V_0} \int e^{-x/\Lambda} (1 - e^{-y/\Lambda}) \, dV_0$$

In our experiment, the 2-prong non-coplanar events should be related to f_1, and all multi-prong events to f_2. Thus the experimental ratio of these two types of events can be compared with the calculated value of f_2/f_1.

The evaluation of the above integrals is easy if one assumes that the proton and neutron are emitted in opposite directions. Thus the integration gives:

$$f_2 = 6\xi^{-3}\left[1 - e^{-\xi}\left(1 + \xi + \tfrac{1}{2}\xi^2\right)\right]$$

$$f_2 = 3\xi^{-3}\left[\tfrac{1}{2}\xi^2 + 3e^{-\xi}\left(1 + \xi + \tfrac{1}{3}\xi^2\right) - 3\right]$$

where $\xi = 2R/\Lambda$ and R is the nuclear radius; $R = 1.3A^{\frac{1}{3}} \cdot 10^{-13}$ cm.

The mean free path Λ is given by (46):

$$\frac{1}{\Lambda} = \frac{3}{8\pi r_0^3}\left[\sigma_{NP} + \sigma_{PP}\right]$$

where σ_{NP} and σ_{PP} are the N-P and P-P scattering cross-sections, and $r_0 = 1.3 \cdot 10^{-13}$ cm is the nucleon

radius.

Λ was calculated for an average neutron energy of 80 Mev(=110 Mev inside the nucleus with a 30 Mev deep potential well)*, and was found to be $\Lambda = 2.02 \cdot 10^{-13}$ cm. With this value of Λ the following values for f_1, and f_2 were obtained:

Nitrogen: $f_1 = 0.12$: $f_2/f_1 = 2.33$
$f_2 = 0.28$

Neon: $f_1 = 0.10$: $f_2/f_1 = 2.70$
$f_2 = 0.27$

The experimental ratios of multi-prong events to 2-prong non-coplanar are:

Nitrogen : 3.3 ± 0.6
Neon : 3.6 ± 0.7

However, it should be stressed that a certain proportion of 2-prong non-coplanar events can be also of the multi-prong type, since neutrons can be emitted from an excited nucleus with an even bigger probability than protons. If we assume these two processes to be of equal probability, the experimental ratios become:

Nitrogen : 8.5

Neon : 7.5

* For simplicity, it was taken that $E_p = E_N$, i.e. $\Lambda_p = \Lambda_N$; because of this the ratio f_2/f_1 is overestimated.

Thus, in both cases the ratio f_2/f_1 is much higher than the calculated one. There are three possible explanations for this discrepancy:

(1) Neutrons accompanying the triggering protons were of smaller average energy than the 80 Mev assumed in the above calculation. This is possible because of the $^1/E$ character of the γ -ray spectrum. The protons were required to have 100 Mev and the quasi-deuterons having high momenta in the same direction as the proton would be favoured. Thus the average neutron energy will be lower. However, this effect was taken into account by assuming 80 Mev for the average neutron energy corresponding to the average proton energy of 100 Mev.

It is difficult to state whether this is a low enough value. This is particularly doubtful in the case of the neon experiment, which was performed with a bremsstrahlung beam of 240 Mev maximum energy. However, complete agreement with the experimental results would require an assumption of as low an average neutron energy as 50 Mev.

This, however, is not in accordance with the energies involved in multi-prong events, if we take into account the binding energies and also the possibility that neutrons are emitted from the residual nucleus.

It should also be added that the data from the counter experiments indicate a higher probability for particles to escape without an interaction than the values obtained in our calculation. For example, Barton and Smith (21), in an experiment using a 280 Mev bremsstrahlung beam, measured the ratio of the single proton counting rate to the number of p-n coincidences, i.e. the ratio $(f_1 + f_2)/f_1$. For E_p = 100 Mev, they obtained for lithium, $(f_1 + f_2)/f_1 = 0.72/0.52 = 1.4$, or $f_2/f_1 = 0.4$. Extrapolating this result to carbon they estimated the probability for a 100 Mev nucleon to escape without interaction to be 35 percent. This leads to a value $f_2/f_1 = 0.55$, which is much lower than our estimation. However, they assumed that the probabilities of the scattering of the proton and neutron were independent of each other. This is not true, since the shorter the distance travelled inside the nucleus by one nucleon, the longer the distance travelled by the other. As an example of the error involved, the calculation of f_2/f_1, for nitrogen gave a value of 1.9 when the scatterings were assumed to be independent. Thus, the disagreement becomes even worse.

(2) If the residual nucleus is left with a high excitation energy, a certain number of multi-prong events will not be due to the nucleon absorption. If this is the case, the excitation energies must be rather high, since the lowest thresholds for reactions in C^{12} and F^{18} are 7.2 and 4.3 Mev, respectively. The excitations of the residual nucleus below these thresholds were impossible to note in the present experiment.

The results obtained for the relative amount of the p-n emission in the counter experiments, can be brought in agreement with our results only if a strong effect of the excitation of the residual nucleus is assumed.

(3) Some other mechanism of γ-ray absorption, resulting in the emission of high energy protons may be the cause of multi-prong events. For example, meson production and reabsorption in the same nucleus would almost certainly result in a higher proportion of multi-prong events. That this effect may be of importance can be inferred from two facts. Firstly, mesons were found (47) to be predominantly absorbed by small groups (2 to 4) of nucleons in the nucleus; thus, a high proportion of emission high-energy protons is possible. Secondly, the number of events, in our results, which contained a high energy proton in addition to the triggering proton is rather high and is difficult to explain on the basis of scattering of the outgoing neutrons on protons, or on the basis of evaporation of the residual nucleus. Particularly if it is remembered

that these protons were almost always not far out of the plane of the triggering proton and the γ-ray. It may be of importance to this argument that 2 events were found (one in neon, and the other in the impurities in helium), which involved two very fast particles in addition to the triggering proton, and both these particles were almost coplanar with the proton. One of these events is shown in Photograph 5, and the other is almost identical to this. It is difficult to find any other explanation of these events but that they were a result of the reabsorption of mesons (e.g. π^+ meson absorbed by a proton-deuteron pair). But this type of meson absorption is probably only of the second order, and therefore, the total effect of meson reabsorption can be much higher.

Another process which would also give a higher proportion of multi-prong events and, in particular, the emission of two high-energy protons, is the absorption of γ-rays by proton-proton pairs (via electric quadrupole).

If one assumes that all events in which two high-energy protons are emitted are due to these two effects, then their relative contribution to the γ-ray absorption

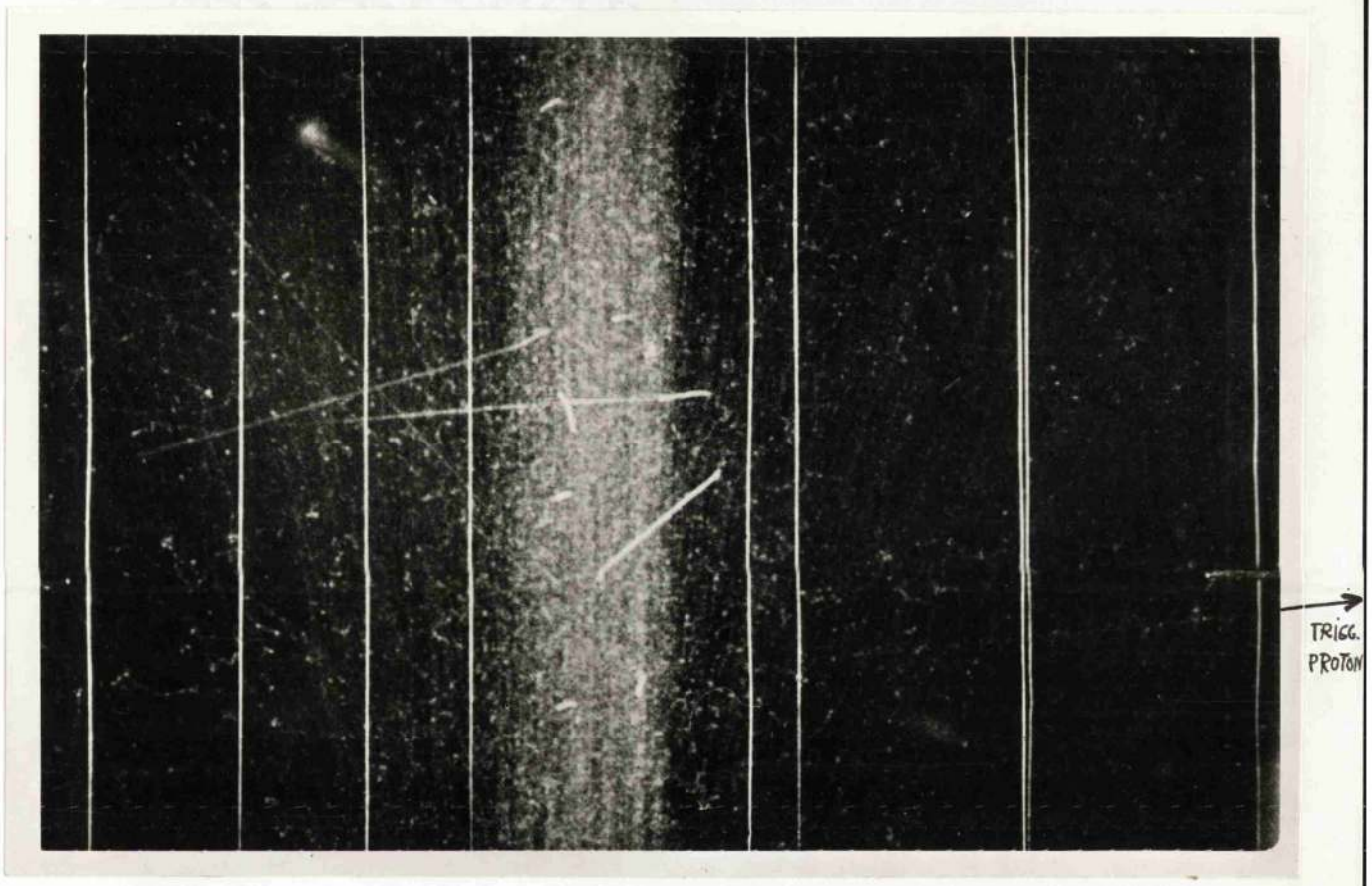

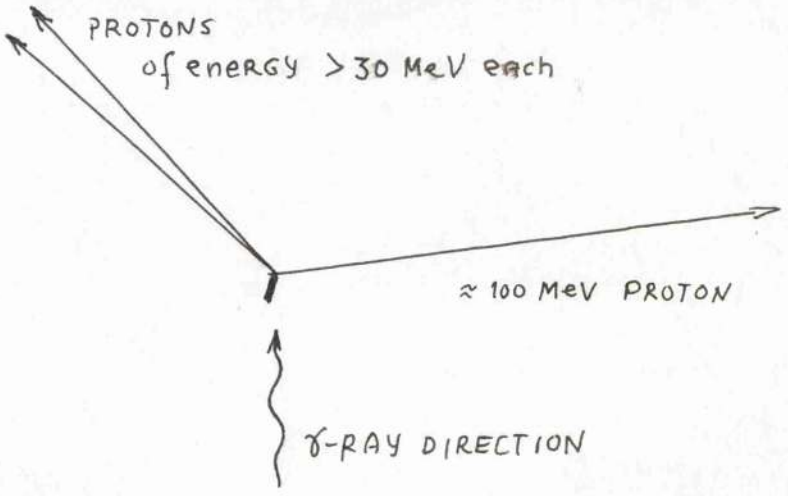

Photograph 5.

See Page 96.

would be higher than 12 percent in Nitrogen and higher than 7 percent in Neon. This estimation does not include the possibility that the second proton can also be often reabsorbed.

In the experiment with helium it was not possible to separate events in which the interaction of the neutron with the residual deuteron was appreciable. It is questionable whether one can even consider such an interaction as being a distinctive process from the γ-ray absorption in a nucleus so tightly bound as helium.

In this case also, there were 5 events (roughly 20 percent) with a high-energy particle nearly coplanar with the triggering proton.

Barton and Smith (21) obtained, for helium, a value of 0.16 for the ratio f_2/f_1. If we assume that our five events are due to the scattering of the outgoing neutrons, we would get a much higher f_2/f_1 ratio, since these events would account only for neutron scattering on protons, and a large angle scattering at that.

Hence, it is difficult to give such an interpretation to these events. It is more probable that they are a direct result of the γ-ray absorption.

One, perhaps the best, way of finding the relative

importance of factors, listed under (1), (2) and (3), seems to be to obtain the angular distributions of protons for each particular type of event. Such data would show whether they are all of the same origin. The statistics attained in the present work are not adequate to derive such data, but the advantage of using the triggered cloud chamber for obtaining it seems obvious.

It is of interest that a certain number of reactions of the (γ ,p) type were found. There are two possible mechanisms for this reaction. One is a direct photo-ejection of a single proton. The other possibility is that the neutron from the disintegrated quasi-deuteron receives such a low energy that it is retained in the residual nucleus. Both of these processes require the existance of very high nucleon internal momenta.

The former process was treated theoretically by Courant (12). Using a square well potential Courant derived the following expression for the cross-section for one proton for photoejection, from a complex nucleus:

$$\sigma = \frac{16}{3}\frac{\pi e^2}{\hbar c}\left(1-\frac{Z}{A}\right)^2 \frac{TW}{(\hbar\omega)^3\left[(\hbar\omega+T)^{1/2}+(\hbar\omega+T-W)^{1/2}\right]}\left(\frac{\hbar}{2MR^2}\right)^{3/2}R^2$$

where T is the kinetic energy of the proton in the nucleus and W is the depth of the potential well; M is the proton mass, and R is the nuclear radius. Assuming a Fermi distribution for the nucleon internal momentum

with Tmax = 22 Mev and W = 30 Mev one gets for the case of nitrogen ($Z = 7$):

$$\sigma \approx 1 \cdot 10^{-30} cm^2$$

This is an order of magnitude smaller than the value obtained in our experiment. It should be noted, however, that Courant's formula was derived for lower γ-ray energies, and it is not certain that it can be applied to higher energies without any modifications. For example, only surface protons (protons at the top of the potential well) were considered in Courant's treatment.

On the other hand, the neutron will acquire an energy lower than 10 Mev in the quasi-deuteron photo-disintegration if this latter has an internal momentum of about 400 Mev/c, (i.e. kinetic energy of 40 Mev), in the same direction as the proton emission (for E_p = 100 Mev, $\theta_p = 50^\circ$).

It is of interest also, that a certain percentage, (12 percent with a large statistical error), of the $He^4(\gamma, p)T$ reaction in helium at energies above 100 Mev was also found. Barton and Smith (21) estimated that 3.5 percent of protons above 100 Mev in their experiment could be due to this reaction.

The absolute values of cross-sections obtained in

our results may have an error of ± 50%. There were two MAIN sources of such a large inaccuracy. Firstly, the energy spread of protons accepted by the telescopes was not precisely determined. Secondly, in some cases, the triggering particle may not have been seen because of poorer quality of photographs; This may be particularly serious in the case of helium, where it was very difficult to observe the triggering particle. Because of the uncertainty in the absolute values it is not possible to check accurately whether the cross-sections for He,N and Ne show A - dependence as predicted by the quasi-deuteron model. The experimental ratios are, within the experimental error, in accordance with such a dependence.

Finally, it should be noted that the recoil energy distributions, listed in Tables 9 and 18 are to be related to the quasi-deuteron internal momentum distributions. The only corrections to be made to the experimental results, are those due to: (a) the $^{1}/E$ nature of the bremsstrahlung spectrum, and (b) to the probability that the residual nucleus evaporates neutrons. Due to the first factor, the high momenta are over-emphasized, and the second is probably of less importance. A method was developed to correct the distribution for the $^{1}/E$ spectrum. The relative probability P(**D**) of the quasi-

-deuteron internal momentum D was divided by a factor proportional to

$$\int_{E_{\gamma MIN}}^{E_{\gamma max}} \sigma(E) \frac{1}{E} dE$$

where $E_{\gamma MIN}$ is the minimum photon energy required to produce a proton of energy E_p at an angle θ from a quasi-deuteron having internal momentum D. This factor was calculated for several proton angles assuming that $\sigma(E)$ is constant. The experimental values for P(D) were then devided by an average of this factor, and a fit to a Gaussian curve was attempted. Unfortunately, the statistics attained in the experiments were not sufficient to derive accurate values for the average quasi-deuteron momenta, but the possibility of deriving this data from the recoil momentum distribution is demonstrated.

APPENDIX.

Author's work in the Institute for Nuclear Sciences - "B. Kidrich", Belgrade.

1. Some development of the diffusion cloud chamber technique.

Done in collaboration with Dr. A. Milojevic and Dr. M. Cerineo, (2A, 3A).

Soon after Cowan (1) demonstrated that a permanently sensitive diffusion cloud chamber was a practical proposition, a work was undertaken in Belgrade with the purpose of developing this technique further. A diffusion cloud chamber was built and its operation under different conditions of vapour and gas filling, and the temperature intervals, was studied.

The chamber was of the cylindrical type, 16 cm. in diameter. It was cooled by means of liquid air, so that the bottom temperature could be maintained between 100 and 140 degrees.

The working conditions of the chamber were studied for pressures in the chamber, from 20 cm.Hg. up to 4 atm. It was found that it could be used for particle detection over this region of pressure, both for air and methane gas fillings. Even electrons were visible down to a pressure of 30 cm.

Particular attention was paid to conditions under which only heavy particle tracks were to be formed. It was felt that such conditions would enable the chamber to be used in experiments where heavy particles would have to be detected in the presence of high background ionization. It was found that when the temperature of the top plate of the chamber was near 0° and that of the bottom below -100° that a discrimination effect appeared. Electron tracks were not readily formed, while the proton and α-particle tracks were very sharp. An electric field did not exert much influence on the chamber operation under these conditions, and the chamber could withstand an ionization several times higher than normally.

An attempt was further made to apply a photo-multiplier tube for the automatic registration of the passage of particles through the sensitive region. For this purpose, a thin layer, approximately 1 cm. high of the sensitive region of the chamber was illuminated by a weak light source (a 25 Watt incandescent lamp). Due to the diffusion of light on the formed droplets, the appearance of a particle track produced a pulse in the photomultiplier. This pulse was then used to

trigger the illuminating system.

The block scheme of the arrangement for the automation of the diffusion chamber is shown in Figure 1A. In the illuminated region of the chamber a weak source of protons (a Po α-source covered with a mica foil) was placed, its intensity being 10 to 15 protons per minute. In order to correlate the photomultiplier pulses with the tracks seen on the photographs, only a small part of the chamber was exposed to the photomultiplier view. Almost on every photograph one could see a proton track crossing this region. One was also able to check directly the photomultiplier operation by looking at the chamber and listening to the operation of a relay which was incorporated in the output of the amplifier; each track was followed by a "click" of the relay. Thus the photomultiplier could be used to take automatic photographs of heavy particle tracks. It was possible to achieve a reasonable good photographs of the tracks, by using a short delay for the illumination, but the electric field had to be present, hence there was a limit to the sharpness of the tracks.

It was important to have a D.C. supply for the permanent light source, otherwise, the photomultiplier

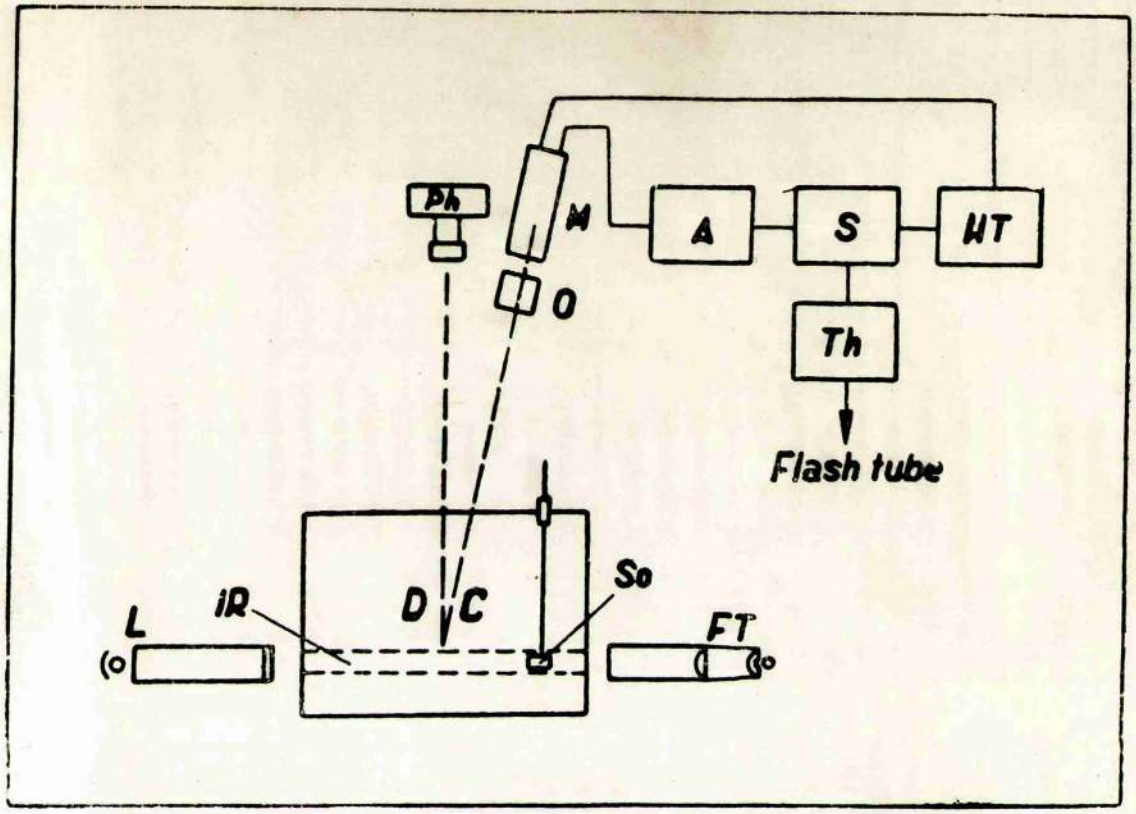

Fig. 1 — Block-scheme of the automatic diffusion cloud chamber.
DC — Diffusion cloud chamber cooled by means of liquid air (1),
So — Source of protons,
FT — Xenon flash tube,
L — Constant light source (incandescent lamp of 25 watts), with collimator and filter,
IR — Illuminated region, ca 1 cm high,
Ph — Photographic camera,
O — Optical system with a segment diaphragm,
PM — Photomultiplier tube (6260),
A — Amplifier,
S — Electronic switch for cutting off the high tension before the flashing of the Xe-tube,
HT — High tension,
Th — Thyratron commanding the flashing of the Xe-tube.

Fig.1A. Block scheme of the automatic diffusion cloud chamber.

would follow the A.C. variation of the source intensity.

The pulses produced in the photomultiplier output were up to 100 mV. in amplitude, and their duration varied between 0.5 and 1 second. The pulse duration was found to depend much on the temperature interval in which the chamber was operated, the pulses being slower at lower temperatures. The pulses due to individual electrons were many times smaller than the pulses due to heavy particles.

This automatic chamber was intended to be applied in the investigation of some reactions with fast neutrons, but no such work has been done yet.

2. Neutrons produced in the bombardment of beryllium by deuterons.

Done in collaboration with F. Borelli (4A).

A measurement of the thin-target yield of neutrons from the $Be^{9}(d,n)B^{10}$ reaction, for deuteron energies from 0.7 to 1.5 Mev, was performed by using 1.5 Mev High Voltage set at the Institute of Nuclear Sciences in Belgrade.

Neutrons were detected with two Hornyak type scintillators, 3 cm. in diameter and 1.5 cm. thick. A 6260 EMI photomultiplier, a cathode follower, a linear

Bell amplifier and an integral discriminator were used. The efficiency of Hornyak scintillator for fast neutrons from 0.5 to 5 Mev is about 1 percent, for -rays it is very low. The geometry of the experiment is shown in Figure 2A. The neutron counters were placed as near to the target as possible, so that the angle of detection was $90^{\circ} \pm 25^{\circ}$ with respect to the deuteron beam. The beam was deflected through 30° by a magnetic analyser. The $Be^{9}(p,\gamma)$ reaction was used for the calibration of the deuteron energy.

Bombarding current was measured with a current integrator having a low impedance input and a precision better than 1 percent. The deuteron beam was collimated with a tungsten foil slit. Beryllium targets, 20-60 Kev thick, were prepared by evaporation of beryllium in high vacuum on to a copper foil of 0.05 mm. thickness. Target thicknesses were determined by weighing on a microbalance.

Figure 1A shows the measured excitation curve (a), together with the curve of Evans et al. (5A) (b) taken at 0°. Resonance at 1,000 Kev is indicated by the shape of the curve. The mean of counts of two detectors were always taken and the curve is a result of many repeated measurements.

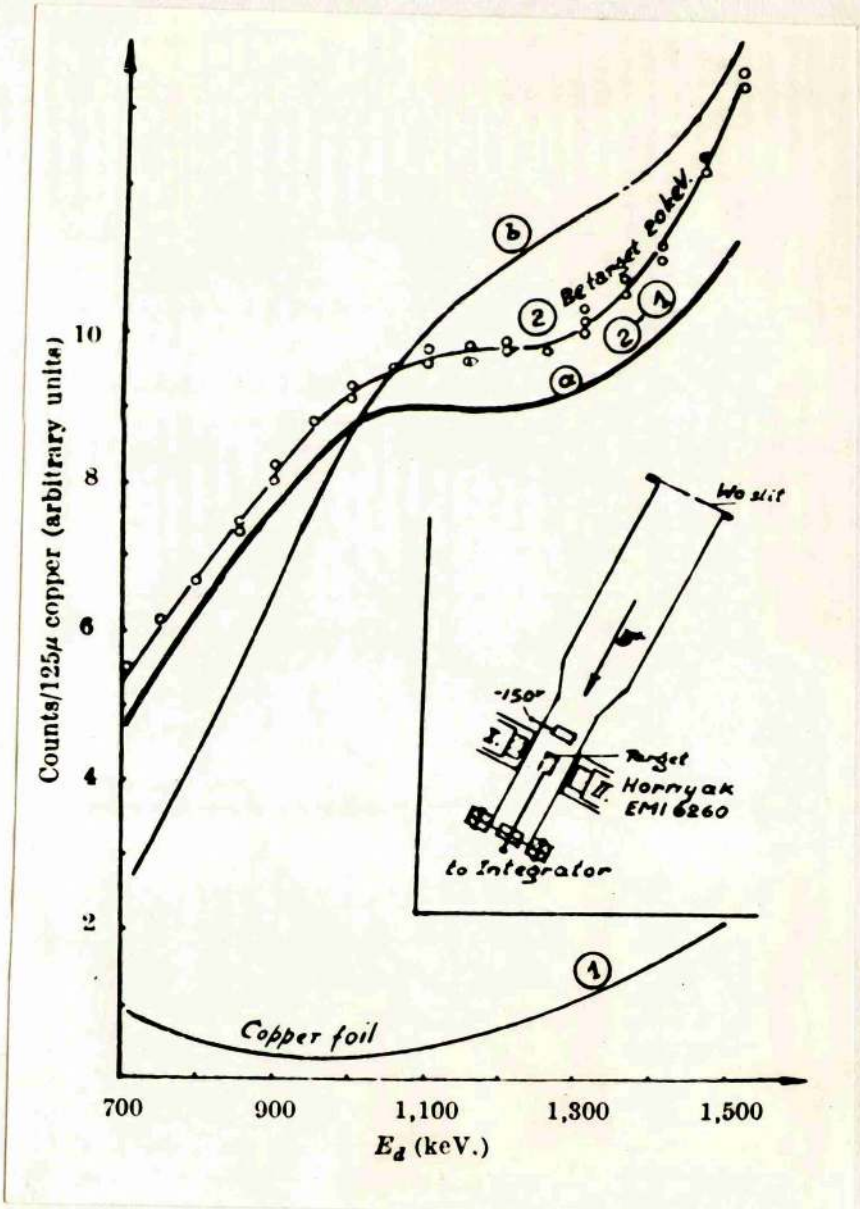

Fig.2A. Excitation curve for $Be^{9}(d,n)B^{10}$ reaction

23. Baranov,P.S.,Goldanskii,V.I., and Roganov, V.S., J.E.T.P.,33,1123,(1958).

24. Chuvillo,J.V. and Schevchenko, V.G., J.E.T.P.,34,593,(1958).

25. Chuvillo,J.V. and Schevchenko, V.G., J.E.T.P.,5,1090,(1957).

26. Whitehead,C.,McMurray,W.R., Aitken,M.J. Middlemas,N., and Collie,C.H., Phys.Rev.,110,941,(1958).

27. Johanson, S.A. Phys.Rev,97,434,(1955).

28. Bazdanov,et al., J.E.T.P.35,322, (1958).

29. Kikuchi,S., Phys.Rev.86,41,(1952).

30. Miller, R.P., Phys.Rev.82,260,(1951).

31. PetersonV.F. and Roos,C.E., Phys. Rev.105,1620,(1951).

32. Schoff,L.F;Marshal,J.F. and Guth,E., Phys.Rev78,733,738,(1950).

33. de Swart,J.J. and Marshak R.E., Phys.Rev.,111,272,(1958).

34. Wilson,R.R., Phys.Rev.,86,125,(1952)

35. Feld,B., Nuovo Cimento,Suppl.2-I, 145,(1955).

36. Austern,N., Phys.Rev.100,1522,(1955).

37. Wilson,R.R., Phys.Rev.104,218,(1956).

38. Gottfried,K., Nucl.Phys.5,557,(1958).

39. Meyer,B.,and Stodiek,W., Rev.Sc.Instrum.24,96,(1953).

40. Birks, J.B.,Scintillation Counters, - (1953).

41. Boreli,F., and Grimeland,B., NuovoCimento,2,336,(1955).

42. Aaron et al. C.I.T.Tables of Range-Energy data. UCRL-12

43. Rutherglen,J., private communication.

44. Atkinson,J.R.,McFarlane,W., Reid,J.M. and Swinbank,P., Nucl.Instrum,1,152,(1958).

45. Lillie,A.B. Phys.Rev.87,716,(1952).

46. Serber,R., Fernback,S., and Taylor,T.B., Phys.Rev.75,352,(1949).

47. Bleuler,K., Terreaux,C.H., Helv.Phys.Acta,27,489,(1954).

(1A) Cowan,A.W., Rev.Sc.Instrum.21,991,(1950).

(2A) Milojevic,A., Cerineo,M., and Lalovic,B., Bull.Inst.Nucl.Sc.,Belgrade, 3,23, (1953).

(3A). Lalovic,B., Milojevic,A., and Cerineo,M., Bull.Inst.Nucl.Sc.Belgrade, 4,97,(1954).

(4A) Boreli,F., Lalovic,B., Nature,176,1021,(1955).

(5A) Evans,J.E. Malick,C.W. and Risser,I.R., Phys.Rev.75,1161,(1949).